

Effect of Nanofibers on the Mechanical Properties of Epoxy hybrid Syntactic Foam

A Major Project Report submitted in partial fulfillment for the award of the degree

Of

MASTER OF TECHNOLOGY

IN

POLYMER TECHNOLOGY

Submitted by

BARIYA QAYYUM

(Roll No: 2K13/PTE/04)

Under the able guidance Of

Dr. PRASUN K ROY

SCIENTIST 'E'

CENTRE FOR FIRE EXPLOSIVE AND FIRE SAFETY (CFEES)

DEFENCE RESEARCH&DEVELOPMENT ORGANISATION (DRDO)

TIMARPUR DELHI 110054

&



Prof. Dr. D. KUMAR

HEAD OF DEPARTMENT

DEPARTMENT OF APPLIED CHEMISTRY AND POLYMER

TECHNOLOGY

DELHI TECHNOLOGICAL UNIVERSITY

(FORMERLY DELHI COLLEGE OF ENGINEERING)

Delhi-110042



CERTIFICATE

This is to certify that the M.Tech major project entitled “*Effect of Nanofiberson the Mechanical Properties of Epoxy hybrid Syntactic Foam*” has been submitted by *BariyaQayyum*, for the award of the degree of “*Master of Technology*” in *Polymer Technology* is a record of bonafide work carried out by her. Bariyahas worked under our guidance and supervision and fulfilled the requirements for the submission of the thesis. The project work has been carried out during the session 2015.

To the best of our knowledge and belief the content therein is her own original work and has not been submitted to any other university or institute for the award of any degree or diploma.

Prof. Dr. D. KUMAR
Head of Department
Department of Applied Chemistry
& Polymer Technology
Delhi Technological University,
Main Bawana Road, Delhi-110042

Dr. P. K. ROY
Sc' E'
Centre for Fire, Explosive & Environment Safety
(CFEES)
Defence Research & Development Organization
Timarpur, Delhi-110054

ACKNOWLEDGEMENT

I express my sincere thanks and deep sense of gratitude to my supervisors Dr. P.K.Roy (Scientist 'E', Centre for Fire, Explosive and Environment Safety (CFEES), DRDO) for his inspiring guidance, constant encouragement and motivation throughout the course of this work. To him I owe more than words can say and Dr. D. Kumar (Professor and Head of Department, Dept of Applied Chemistry D.T.U) for guiding me and helping me in all ways throughout my course work.

I take this opportunity to thank the management of CFEES, DRDO for giving me this opportunity to carry out this project work in their esteemed laboratory. It was a privilege to work under the esteemed guidance of MrA.V.Ullas.

I would like to express my profound gratitude to all the faculty members and the non-teaching staff of Department of Applied Chemistry and Polymer Technology D.T.U. for helping me in all the related problems during the entire duration of M.Tech.

I want to thank MrsSurekhaParthsarathy,Mr. Saurabh Chaudhary, for their immense support and guidance that helped me in completing the project

I thank all the members of Centre for Fire Explosive and Environment Safety (CFEES) for their kind cooperation.

I thankfully acknowledge my family members and friends whose inspiration and motivation brought me to the completion of this project. This was a great learning experience and I will cherish it throughout my life.

DATE:

(BARIYA QAYYUM)

UNDERTAKING

I declare that the work presented in this thesis titled “Effect of Nanofibers on the mechanical Properties of Epoxy hybrid Syntactic Foam”, submitted to the Department of Applied Chemistry & Polymer Technology, is an authentic record of my own work carried out under the supervision of Dr. D. Kumar, Head of Department, Department of Applied Chemistry & Polymer Technology, Delhi Technological University & Dr. Prasun K Roy, Scientist-E, (CFEES) DRDO, Delhi.

This report does not contain any work which has been submitted for the award of any other degree either of this university or any other university, to the best of my knowledge, without proper citation.

Date:

Place: DTU, Delhi

(Signature of Candidate)

CONTENTS	Page no
LIST OF FIGRUES	ix
LIST OF SCHEMES	xii
LIST OF TABLE	xiii
ABSTRACT	xiv
CHAPTER 1	1
INTRODUCTION AND LITERATURE SURVEY	1
1.Introduction	1
1.1. syntactic foam	3
1.1.1. Matrices used in syntactic foams	4
1.1.2. Microsphere in syntactic foams	4
1.1.3. Structure of syntactic foams	5
1.2. Epoxy syntactic foam	6
1.2.1. Thermosetting epoxy resins	7
1..3. Fiber reinforced syntactic foams	9
1.3.1. Nanofiber reinforced syntactic foams	9
1.3.2. Nanofiber	9
1.3.2.1.Electrospinning	10
1.3.2.2. Factor Affecting Properties of electrospun fibers	11
1.3.2.2.1. Molecular Weight ,Viscosity and Concentration	11
1.3.2.2.2. Solution conductivity	11
1.3.2.2.3. Effect of Voltage	11
1.3.2.2.4. Flow Rate	12
1.3.2.2.5. Diameter of Needle Electrode	12

CONTENTS	Page No
1.3.2.2.6. Distance between the collector and the tip of the syringe	12
1.3.2.3. Mechanism of fiber formation in Electrospinning	12
1.3.2.4. Application of syntactic foams	14
1.4.Aims and Objectives	16
CHAPTER 2	17
EXPERIMENTAL	17
2.1. Introduction	17
2.2. Materials	17
2.3. Electrospinning set up	17
2.4. Preparation of polystyrene nanofibers	19
2.5. Preparation of nylon 6 nanofibres	20
2.6. Fabrication of neat and nanofibre reinforced syntactic foam	20
2.6.1. Fabrication of neat syntactic foam	20
2.6.2. Fabrication of nanofibre reinforced syntactic foam	20
2.6.2.1. By random reinforcement	20
2.6.2.2. Oriented reinforcement	22
2.7. Density Determination	23
2.8. Void volume	23
2.9. Characterization of fibres	23
2.9.1. Structural characterization	23
2.9.1.1 Scanning Electron Microscopy	23
2.9.2. Thermal Characterization	25

2.9.2.1. Thermogravimetric Analysis	25
2.9.2.2. Differential Scanning Calorimetry	26
2.10. Mechanical Testing	26
2.10.1. Compression Testing	26
2.10.1.1. Compression testing of fibers reinforced syntactic foam	28
2.10.1.1.1. Polystyrene nanofibers syntactic foam	28
2.10.1.1.2. Nylon6 nanofibre syntactic foam	29
2.10.1.2. Energy Absorption Mechanism in syntactic foam	29
2.10.1.3. Flexural testing	31
CHAPTER 3	32
RESULT AND DISCUSSION	32
3.1. Syntactic foam	32
3.2. Glass microballoons	33
3.3. Neat syntactic foam	33
3. 3.4. Mechanical Testing	34
3.4.1. Compression Test	34
3.4.1.1. Effect of volume ,fraction on compressive properties of syntactic foam	37
3.5. Nanofibers reinforced syntactic foam	38
3.5.1. Polystyrene nanofibers	38
3.5.1.1. Effect of Concentration on the polystyrene fiber morphology	39
3.5.1.2. Effect of flow rate on polystyrene nanofibers morphology	40
3.5.1.3. Fiber size distribution	41
3.5.1.4. Thermal characterization	42
3.5.2. Nylon 6 nanofiber	43

3.5.2.1. Effect of Concentration on fiber morphology	43
3.5.2.2. Effect of flow rate on fiber morphology	44
3.5.2.3. Fiber size distribution	45
3.5.2.4. Thermal Characterization	46
3.6. Nanofibers reinforcement in syntactic foam	47
3.6.1. Density Determination	48
3.6.2. Mechanical testing of nanofiber reinforced syntactic foam	49
3.6.2.1. Polystyrene nanofiber reinforced syntactic foam	49
3.6.2.1.1. Compression Testing	49
3.6.2.2. Nylon 6 nanofiber reinforced syntactic foam	51
3.6.2.2.1. Compression Testing	51
3.6.2.2.2. Energy Absorption	53
3.6.2.2.3. Flexural Testing	54
3.7. Thermal Characterization of syntactic foam	56
CHAPTER 4	59
SUMMARY AND CONCLUSIONS	59
CHAPTER 5	61
REFERENCES	61

TABLE OF FIGURES

FIGURES	PAGE NO
Fig 1.1: Schematic representation of (a) two-phase and (b) three-phase structures of syntactic foam	6
Fig 1.2: Schematic diagram of electrospinning process	11
Figure 1.3: Schematic diagram illustration of the Taylor cone formation	13
Fig 1.4: HOV Alvin and ROVs Janson used for deep see exploration. Photo courtesy (NOAA)	15
Fig 2.1: Setup of an electrospinning unit (ESPIN-NANO (PHYSICS EQUIPMENTS CO.))	18
Fig 2.2: Steps for preparation of syntactic foam containing nanofibers	21
Fig 2.3: Layered nanofibre reinforced syntactic foam specimen	22
Fig 2.4: Scanning electron microscope	25
Fig 2.5: Thermogravimetric analysis	25
Fig 2.6: Universal Testing Machine (UTM)	27
Fig 2.7: Arrows shows the loading direction and black lines specify the preferred orientation of fibers	29
Figure 2.8: Compression stress-strain response of syntactic foam	30
Fig 2.9: sample of flexural testing	31
Fig 3.1: Representative image of neat syntactic foam	34

Fig 3.2: Representative stress strain curve of syntactic foam	35
Fig 3.3: SEM image of compressed syntactic foam	36
Fig 3.4: Compressive stress strain curve of neat syntactic foams containing varying HGM loadings	37
Fig 3.5: Comparison of compressive strength of neat syntactic foams at varying HGM volume fraction	38
Fig 3.6: Effect of concentration on the surface morphology of polystyrene nanofibres at different concentrations: (a) 5%a (w/v) (b) 10 %s(w/v) (c) 15 %d(w/v) (d) 20 %f(w/v)	40
Fig 3.7: Effect of flow rate on surface morphology of polystyrene nanofibers	41
Fig 3.8: Fiber size distribution at flow rates (a) 0.1 ml/hr (b) 1 ml/hr (c) 3ml/hr (d) 5ml/hr	42
Fig 3.9: TG-DTG traces of polystyrene nanofiber	43
Fig 3.10: Effect of concentration on the surface morphology of nylon6 nanofibres at different concentrations: (a) 5% a(w/v) (b) 10 %s(w/v) (c) 15 %a(w/v) (d) 20 %a(w/v)	44
Fig 3.11: Effect of flow rate on surface morphology of nylon6 nanofibers	45
Fig 3.12: Fiber size distribution of nylon 6 nanofibers	46
Fig 3.13: TGA-DTG of nylon6	47
Fig 3.14: DSC trace of nylon 6 nanofibre	47
Fig 3.15: Compression stress strain curve of PSSF40 containing 0-4vol% PSNFs	50
Fig 3.16: Comparison of compressive strength and modulus of SF40 at different nanofibre loadings	50
Fig 3.17: Fiber reinforced syntactic foam	51
Fig 3.18: Compressive stress strain curve of SF40N25 at different orientations of nylon 6	52

Fig 3.19: Compression strength and modulus of syntactic foams containing nylon 6	52
Fig 3.20: The photographs of compression tested samples (a) perpendicular, (b) parallel are presented (arrows indicate direction of loading)	53
Fig 3.21: Influence of fiber arrangement on the toughness of SF40N25	54
Fig 3.22: SEM image of specimen after flexural test	54
Fig 3.23: Flexural stress strain graph of SF40 and SF40N25	55
Fig 3.24: TGA and DTG traces of syntactic foams at different volume fractions (a) 40%, (b) 50%,(c) 60%. Solid lines represent TGA and dotted lines represent DTG traces	57

LIST OF SCHEMES

SCHEMES	PAGE NUMBER
Scheme 1: Synthesis of diglycidyl ether of bisphenol A(DGEBA)	7
Scheme 2: Reaction scheme of primary amine of TETA with epoxy group	8

LIST OF TABLES

Table 2.1: Properties of epoxy and TETA	17
Table 2.2: Various compositions and designation of neat and nanofibers reinforced syntactic foam	21
Table 3.1: Properties of Microballoons	33
Table 3.2: Experimental and theoretical density of neat and fiber reinforced syntactic foam	48
Table 3.3: Flexural strength and modulus of neat and nylon6 reinforced syntactic foam.	55
Table 3.4: Characteristic decomposition temperatures of samples	58

ABSTRACT

Syntactic foams are a class of materials that consists of hollow spaces inside a solid shell. Owing to the presence of hollow spaces, they are structurally light-weight. This permits their usage in applications where weight is a constraint. However, an inherent disadvantage of such materials is their low mechanical strength (a property attributed to their structure). To do away with this problem, fillers can be added but with an associated problem of increasing the weight. This project is an attempt to improve the mechanical properties of epoxy/HGM syntactic foams by reinforcing them with nanofibrous fillers of polystyrene and nylon 6 which have in turn prepared by electrospinning. Nanofibre webs being very light compared to their micron sized counterparts allows sufficient saving in weight along with providing necessary strength. This thesis focuses on establishing the effect of increasing concentration of the polymer on the morphology of the electrospunfibers. The effect of introducing these fibers at different volume fractions on their compressive and flexural properties have also been explored in this project.

CHAPTER 1

INTRODUCTION AND LITERATURE SURVEY

1. Introduction

Lightweight materials with high strength and stiffness are the need of the hour. These lightweight materials are used in those areas where weight is a constraint but the strength and structural integrity cannot be compromised with. As such they are used in areas of aerospace and marine applications for the construction of light weight aircrafts, submarines respectively. The fabrication of this class of materials is a new field and is characterized by the presence of hollow spaces packed tightly in a matrix which may be of metal, ceramic or polymeric. The presence of hollow spaces is mandatory for the fabrication of such type of materials because this is what which gives the materials light weight and which the sole characteristic of such materials is. The idea behind the development of such materials is to obtain extremely light weight but strong materials. Apart from providing the necessary strength requirements, these materials also serve as good moisture resistant and possess fair dielectric strength. The inspiration to make such materials comes from the traditional foams which are very light in weight but also possess poor mechanical properties. The materials are similar in construction to ordinary foams but unlike foams possess good mechanical strength. These materials resemble ordinary foams that are very light weight and contain open spaces which are a result of chemical reaction but in these materials, the hollow spaces are not created chemically but is the result of deliberate introduction of hollow spherical microspheres enclosed in shell. This is what gives these materials a unique class known by the name of syntactic foams.

LITERATURE SURVEY

The large number of studies have been published on the use of glass microspheres in syntactic foams [1, 2] and carbon nanofibre reinforced syntactic foams [3, 4]. Many processing techniques have been discovered by researchers for the creation of reinforced syntactic foams[5]. Methods developed in these studies have been used in the present study to accomplish minimal air entrapment and proper wetting of microballoons, fillers and resin so that void content is minimized and a strong resin-microballoons interface is achieved.

Syntactic foams were reinforced by using nanoclay[6, 7]. It was indicated in the report that nanoclaysignificantly enhanced tensile strength and toughness with delayed crack instigationand growth. The enhancement in thestrength was due tothe reinforcing effect of the nanoclay particles. Theadditionofnanoclay created large amount of interface between nanoclay particles and the matrix resulting in increase in theamount of energy required to de-bond the interfaces betweenthe glass microballoons, Nanoclay particles, and matrix resin. However,the incorporation of nanoclay reduced the tensile modulus because of a large increase in fracture strain and toughness of syntacticfoams. In addition, increase in strength was followed byincrease in the stiffness and brittleness, makingdamagetolerance properties poor.Bunn et al[8] have stated the compressive properties of syntactic foams made from phenolic microballoons with different volume fractions. As the microballoons volume fraction was increased, a decrease in compressive strength was also observed. Compressive properties of these foams were found tobe relatively poor when compared with foams fabricated from glass microballoons. With microballoons volume fraction of 0.553, compressive strength of 28 MPa and a compressive modulus of approximately 1400 MPa, was obtained, which indicates a good load absorption capability but low compressive strength.Syntactic foams composed of epoxy resin matrix and low density (220 kg/m³) glass microballoons show damage tolerant properties due to the low strength of microballoons. Weak strength of microballoons make them to fracture under the applied load and retain the damage localized. An enormous amount of load energy is captured in the crushing of

microballoons with application of load. Though high density microballoons foams (460 kg/m³) are relatively brittle, they have a lower energy absorption capacity. High density foams tend to fail disastrously soon after the yield stress, which is unwanted for applications requiring high damage tolerance[37].

1.1. Syntactic foams

Syntactic word is derived from a Greek word *syntaktikos* meaning “to arrange together”. The term ‘foam’ is used because of the cellular nature of the material.

Syntactic foams are physical foams in which foaming is achieved by the addition of hollow particles made up of polymers, glass or metals. ASTM defines it as “a material consisting of hollow sphere fillers in a resin matrix”[9]. They are lightweight materials with low density, high specific strength targeted for use in marine, aerospace and such areas where weight is a constraint. They are also known as foam composites since the hollow spheres can be regarded as reinforcements in polymer matrix. Syntactic foams, also known as foam composites are nowadays widely being used as a replacement of heavier materials with no compromise in their mechanical properties when compared to their heavier counterparts. Regardless of the above fact, they find themselves suitable to a wide range of applications designed especially for them. Beyond the limits of the sky to the depths of the ocean there is no such area where they cannot apply themselves to. The aircrafts nowadays require lightweight materials without compromising on the stringent requirements as far as the safety is concerned and so are the underwater jets and submarines which require help in order to counterbalance their own weight, derive immense help from these novel syntactic foams. Foams, as they are called, consist of hollow spaces or voids in between the matrix which plays a crucial role in providing the foams their uniqueness. Generally they are tertiary systems comprising of matrix, hollow microspheres and sometimes voids also adding to their structure.

1.1.1. Matrices used in Syntactic Foams

The matrices used in syntactic foam include polymers[10], metals[11] or ceramics. Thermoplastic and thermosetting polymers have been employed to fabricate syntactic foams. The important thermosetting resins used are epoxies[12], phenolics[13], vinyl esters[14], bismaleimides[14], unsaturated polyesters, and polyurethanes[15]. Examples of thermoplastic resin matrices used include polyethylene, polypropylene[16], polystyrene, and nylons. Syntactic foams are mainly prepared by using thermosetting matrices because of the favourable processing conditions, i.e., avoiding breakage by gently blending the hollow microspheres with thermoset precursors of very low viscosity. From the processing viewpoint, thermosetting syntactic foams have many advantages compared with thermoplastic ones. For example, thermosetting syntactic foams can be processed at much lower temperatures compared with thermoplastic syntactic foams, thereby reducing the material and energy costs for processing. Also, thermosetting resins have less solvent sensitivity and are not negatively affected by cleaning solutions. Nevertheless, some attempts have been made to process syntactic foams with a thermoplastic matrix by using a solvent, or even by using a twin-screw extruder.

1.1.2. Microspheres in Syntactic Foams

Hollow microspheres give the syntactic foam its low density, high specific strength, and low moisture absorption. Microspheres may comprise glass[17], polymer, carbon[13], ceramic[11], or even metal. Bio based reinforcements are now being chosen as opposed to polymeric materials. Shah, D. U., F. Vollrath, et al. demonstrated the use of silk cocoons as a natural microballoons filler in polyurethane foams[18]. Other terminologies are used in the literature to describe microspheres (e.g., microballoons, cenospheres). All these terms are intermittently used throughout this report to indicate hollow microspheres. The microspheres have a burst pressure sufficient to withstand the forces imposed upon them during the

formulation, mixing and dispensing processes. Properties such as high temperature resistance, good strength-to-weight ratios, clean surface chemistry, low thermal conductivity and low dissipation factor make microballoons an important reinforcing material in these composites.

1.1.3. Structure of Syntactic Foams

Syntactic foams are usually tertiary systems because the matrix and microspheres are usually composed of different materials. They are classified as two-phase systems and three-phase systems. The close-packed arrangement of hollow microspheres in the matrix gives rise to two-phase syntactic foams. The two-phase structure is schematically shown in Figure 1.1(a). During the processing of syntactic foams, air entrapment is possible, which leads to voids in the foam structure. In some other cases, a thin film of resin may surround the cluster of microballoons so that the resin cannot penetrate into the cluster, leaving an empty space in between the microspheres. Sometimes, depending upon the application, voids are intentionally incorporated to obtain lower density. The existence of voids makes syntactic foams a three-phase system (unlike conventional polymer foams which are binary). The three-phase structure is shown schematically in Figure 1.1(b). Thus, two-phase syntactic foams consist of hollow microspheres dispersed in a resin, whereas three-phase syntactic foams comprise hollow microspheres dispersed in a resin containing finely dispersed air bubbles.

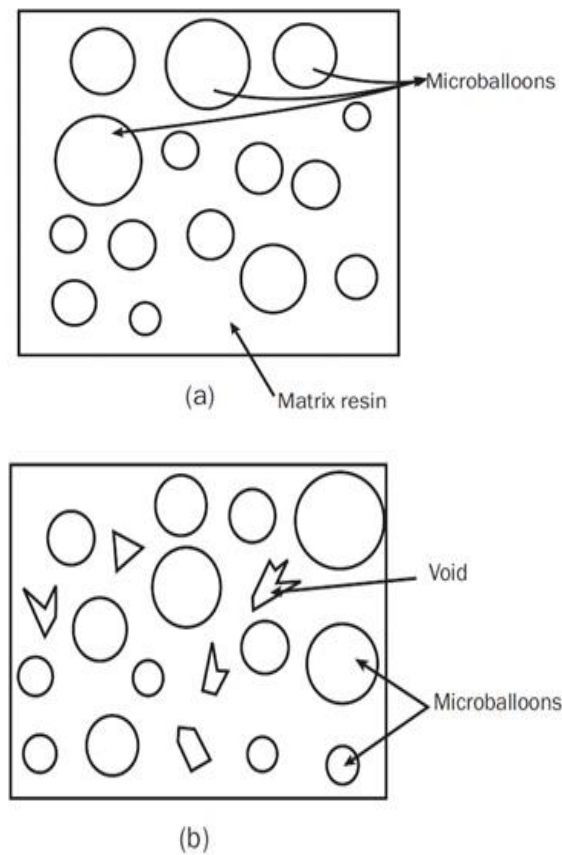


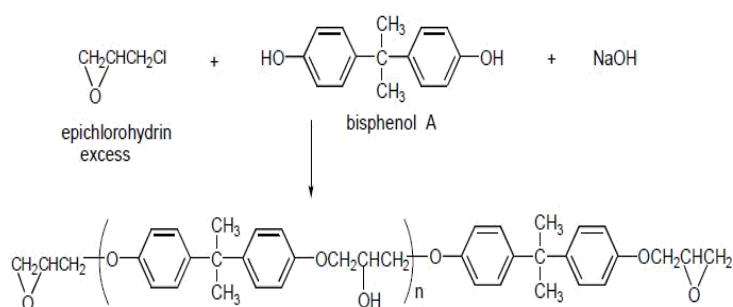
Fig 1.1:Schematic representation of (a) two-phase and (b) three-phase structures of syntactic foam.[9]

1.2. Epoxy syntactic foam

The properties of syntactic foams are very much dependent on the nature of polymer matrix, concentration of the matrix, type of curing agents and type of microballoons used. Epoxy resin is one of the most commonly used matrix because it can produce a syntactic foam which can be easily formulated in various ways to give the desired end product with higher strength and stiffness ,thermal and environmental stability, creep resistance and lower shrinkage and water resistance respectively. Epoxy resin with different variety of microballoons has been used to process syntactic foams. Epoxy syntactic foams with glass polystyrene,carbon, phenolics, and mineral microballoons have been reported.

1.2.1. Thermosetting epoxy resins

Epoxy resins are one of the most important classes of thermosetting polymers. The resin network has many desirable properties which include high tensile strength, excellent chemical and corrosion resistance and good dimensional stability [19, 20]. As a result, these materials are widely used for applications such as matrix for syntactic foams and advanced composite materials [23-25]. Polyepoxide, known commonly as “epoxy” is a thermosetting polymer formed as a result of reaction between an epoxide “resin” with polyamine “hardener”. Commercial epoxy resins contain aliphatic, cycloaliphatic or aromatic backbones. They are prepared from either epichlorohydrin or by direct epoxidation of olefins with peracids. The most important intermediate for epoxy resins is the diglycidyl ether of bisphenol A (DGEBA), which is synthesized from bisphenol A and excess epichlorohydrin as per shown in the scheme 1.2.

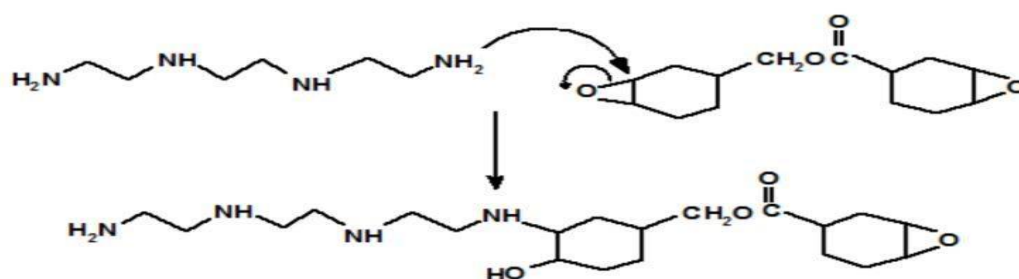


Scheme 1.1: Synthesis of diglycidyl ether of bisphenol A (DGEBA)

The epoxide ring can react with chemicals with different structures, especially those that have activated hydrogen atoms such as alcohols, amines and carboxylic acids, to mention a few. Treatment of epoxy resins with these agents results in formation of three dimensionally insoluble and infusible networks. The choice of curing agents depends on the required physical and chemical properties, processing methods and curing conditions which are desired. Epoxy resins can be cured with either catalytic or co-reactive curing agents who function as initiators for epoxy ring-opening homopolymerization.

Among chemicals which have the potential to act as curing agents, the primary and secondary amines are the ones which are most commonly employed. Primary amine functionality reacts with an epoxy group to produce a secondary amine and a secondary alcohol. The secondary amine can further react with an epoxy group to form a tertiary amine. Commercial hardeners generally consist of polyamine monomers, a typical example being triethylenetetramine (TETA). Each amine functionality can react with an epoxide group, so that the resulting polymer is heavily cross linked, and results in a formation of a rigid and strong structure. For the present study, a cycloaliphatic epoxy resin was chosen due to its potential applicability in different areas and more importantly its UV stability, in view of the absence of light absorbing phenyl rings.

A reaction scheme representing the reaction between the primary amine functionality of TETA with epoxy group is shown in figure 1.2. This process is also referred to as "curing", and can be controlled through proper choice of temperature, type of resin and hardener, and the ratio of said compounds. The curing process, which is exothermic, can take minutes to hours for completion. Some formulations benefit from heating during the cure period, whereas others require time and ambient temperatures



Scheme1.2: Reaction scheme of primary amine of TETA with epoxy group of cycloaliphatic epoxy resin.

1.3. Fibre reinforced syntactic foams

Syntactic foam has been reinforced with conventional fibres lately to obtain improved properties without increasing the weight of the foams. Traditional fibres such as glass fibre[21], short carbon fibre[22], Kevlar [23], etc. has been added as a filler in both thermoplastic and thermosetting matrix. Results have shown that addition of fibres leads to an enhancement in the mechanical properties of the composite. The fibres when dispersed uniformly in the matrix act as distributors of stress which leads to the improved properties of the composites. Fibres, if used as fillers must be spread evenly within the matrix otherwise agglomeration of fibres in any area, decrease the strength. Improper fibre wetting by the resin causes fibre pullout and deteriorate the mechanical properties. In addition to nanofibers, nanoclay, graphene[24] platelets have been added into syntactic foams and the results are reported in the literature.

1.3.1. Nanofibers reinforced syntactic foams

Nanofibres possess the advantage of being lighter when compared to their conventional counterparts. As such they have a tremendous potential to be used as a filler material in enhancing the properties of syntactic foams without adding to its weight. Very little literature is available concerning the use of nanofibres except the use of carbon nanofibre which has been as filler in fabrication of syntactic foams. The scarce amount of data available in this field motivated us to prepare polymeric nanofibres and use them as reinforcements.

1.3.2. Nanofibres

Production of nanofibres is a fascinating area and is the focus for good deal of research activity worldwide. The nano prefix is usually applied to materials having dimensions less than 100nm, but in the case of fibres, the limit can be 0.5 μm or even 1 μm . For simplicity all

sub-micron fibres are referred to as nanofibers. The preparation of polymeric nanofibre by means of a method called electrospinning[25, 26] was first patented in 1902 and has gained increasing attention in recent decades. Competing techniques for the production of polymeric nanofibres are melt blowing technology, melt spin production of islands in the sea structured bicomponents fibers with the dissolvable polymer as a matrix and via fibrillation of linear cellular structured fibres such as cellulose into mono sized sub fibres or fibrils as well as drawing with micropipette, template synthesis, phase separation and self-assembly. Despite its limitations such as relatively low productivity, the electrospinning method remains a promising method that enables preparation of nanofibres.

1.3.2.1. Electrospinning

It is a very simple and versatile process by which polymer nanofibres with diameters ranging from a few nanometers to several micrometers (usually between 50 and 900 nm) can be produced using an electrostatically driven jet of a polymer solution (or polymer melt), under a high-voltage electric field to form solid fibres from a polymeric fluid stream (solution or melt) delivered through a millimeter-scale nozzle. Even though the roots of electrospinning lies fairly deep enough but it has gained widespread popularity only in recent times with many research groups working in the field of nanosensors, tissue engineering scaffolds[27, 28], wound dressing materials [29], composites, etc. which demand highly skilled use of nanofibres in all above fields. Moreover, many research groups have spun nanofibres from different polymers such as nylon 6 [30] cellulose acetate, poly (vinyl alcohol)[31, 32], poly acrylonitrile, polyurethanes, polyethylene terephthalate, polystyrene[33], chitosan [34], etc. and many more polymers.

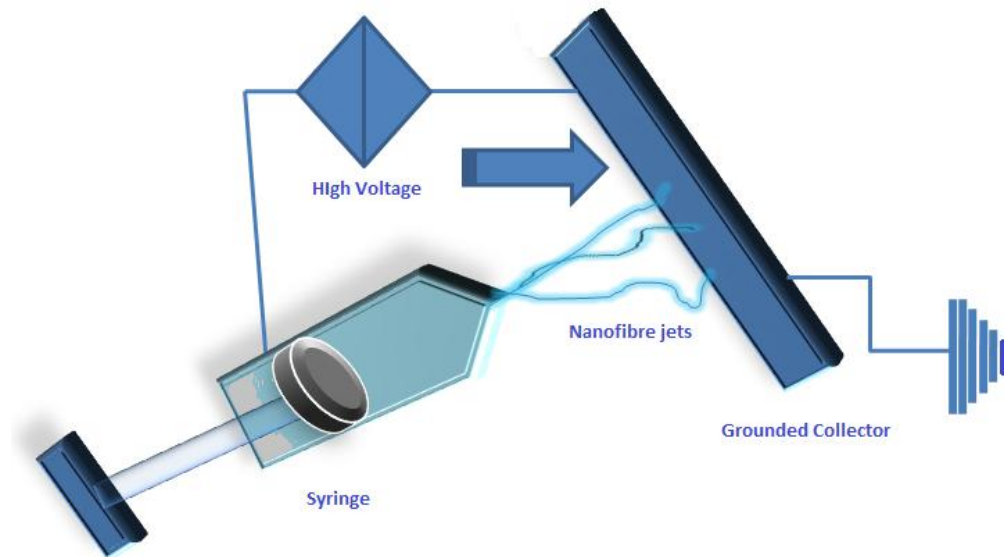


Fig 1.2: Schematic diagram of electrospinning process

1.3.2.2 Factors Affecting Properties of Electrospun Fibers

There are essential factors without which the electrospinnability will be a difficult task.

1.3.2.2.1. Molecular weight, Viscosity and concentration

Molecular weight, which depends on the length of polymer chain, plays a vital role in defining the morphology of electrospun fiber. Polymer chain entanglement also decides whether the electrospinning jet breaks up into small droplets or continuous fibres. At lower viscosity, the higher amount of solvent molecules and less chain entanglement will mean that surface tension has dominant influence along the electrospinning jet beads rather than smooth fibre. Higher the molecular weight higher will be the entanglement polymer chains in solutions which result in increment in viscosity of solution, smooth fibre will be obtained

1.3.2.2.2. Solution conductivity

Electrospinning involves stretching of the solution caused by repulsion of charges at its surface. If the conductivity of the solution is increased, more charges can be carried by electrospinning jet. The increased charges by the solution will increase the stretching of the solution favors the formation of thinner fibres.

1.3.2.2.3. Effect of voltage

Increase in voltage decreases the fiber diameter. Higher voltage offers the greater probability of beads formation [41]. Thus, we can find that voltage does influence fiber diameter, but the level of significances varies with the polymer solution concentration and on the distance between the tip and the collector [42]

1.3.2.2.4. Flow rate.

The flow rate of the polymer solution is another important process parameter. Flow rate determines the amount of solution available for electrospinning. Generally, lower flow rate is more recommended as the polymer solution will get enough time for polarization. If the flow rate is very high, bead fibres with thick diameter will form rather than the smooth fibre with thin diameter owing to the short drying time prior to reaching the collector and low stretching forces.

1.3.2.2.5 Diameter of needle electrode

Smaller the diameter reduces the clogging as well as the diameter of the Electrospun fibers.

1.3.2.2.6. Distance between the Collector and the Tip of the Syringe

The fiber diameter and morphologies can also affect by the distance between the collector and the tip of the syringe. If the distance is too short, the fiber will not have enough time to solidify before reaching the collector, Dryness of the solvent from the electrospun is very important so optimum distance is recommended. Yuan et al. [43] demonstrated that increasing the distance give more time for the solvent to evaporate and for the charged fluids to split more time

1.3.2.3 Mechanism of fiber formation in electrospinning

The mechanism of fibre formation in electrospinning is governed by two prime factors i.e., the surface tension of the polymer solution and the magnitude of the electrostatic charges formed on the surface of the drop as a consequence of the generation of a high potential difference, although other factors such as concentration of solution, viscosity, distance, etc.

also play a major role. To summarize the fibre forming process, the following steps need to be taken into account.

- The surface of the polymer droplet held by its own surface tension at the tip of the needle electrode.
- The interaction of the electric charges in the polymer droplet with the external electric field causes the droplet to assume a conical shape, known as **Taylor cone**.
- When the surface tension of the fluid can be overcome, the droplet becomes unstable and a liquid jet is ejected out.
- The travelling liquid jet stream is subject to two opposing forces.
 - ❖ Electrostatic repulsion of the charges in the jet tends to increase its surface area.
 - ❖ The surface tension of the polymer solution tends to reduce the total surface of the jet which causes the jet to break up into droplets.
- Which of these two opposing effects prevails, depend on the viscosity and surface tension of the polymer solution.

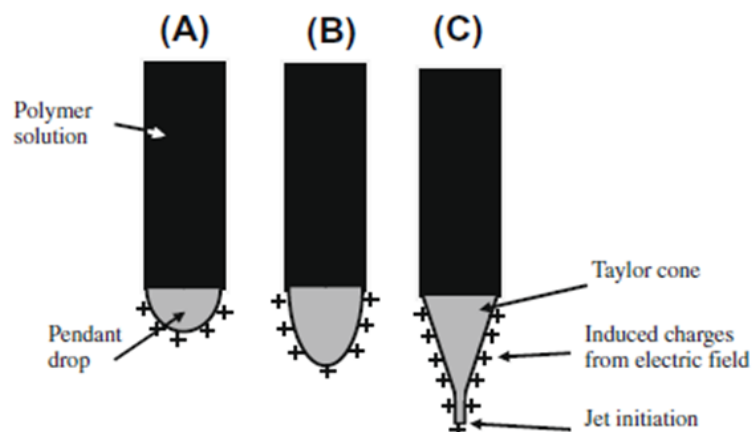


Figure 1.3: Schematic diagram illustration of the Taylor cone formation[35].

- (a) Surface charges are induced in the polymer solution due to the electric fluid.
- (b) Elongation of the pendant drop

(c) Deformation of the pendant drop to the form the Taylor cone due to the charge repulsion. A fine jet initiate from the cone.

1.3.2.4. Application of syntactic foam

Syntactic foams are finding applications in fields that are as diverse as deep sea vehicles, space vehicles, air craft, snow skis, soccer balls and thermal insulation in under water pipelines. Based on the properties, application of syntactic foams can be divided into three categories which are given below.

a) Compressive properties: Syntactic foams are lightweight porous composites that are made by incorporation of HGMs while keeping the compressive strength high as the stiffness of glass microsphere is high which makes it load bearing element under compression. Because of hydrostatic compression encountered by submarine and under water unmanned vehicles, the properties of syntactic foams are effectively used here. The National Oceanic and Atmospheric Administration (NOAA) uses Alvin and Janson underwater vehicles such as Human Occupied Vehicle (HOVs) [36], Remotely operated vehicles (ROVs), Autonomous underwater vehicles (AUVs) that are made of syntactic foams to withstand the extreme pressure thousands of meter below the ocean surface for the purpose of deep sea exploration. The Deep Sea Challenger, used by James Cameron for the exploration of Mariana Trench, was made of reinforced syntactic foam containing fibres and hollow particles in an epoxy resin matrix. The syntactic foam was specifically designed for this submarine that went to the deepest part of the ocean. The syntactic foam structure of the HOVs, ROVs and Challenger craft as shown in figure 1.4.

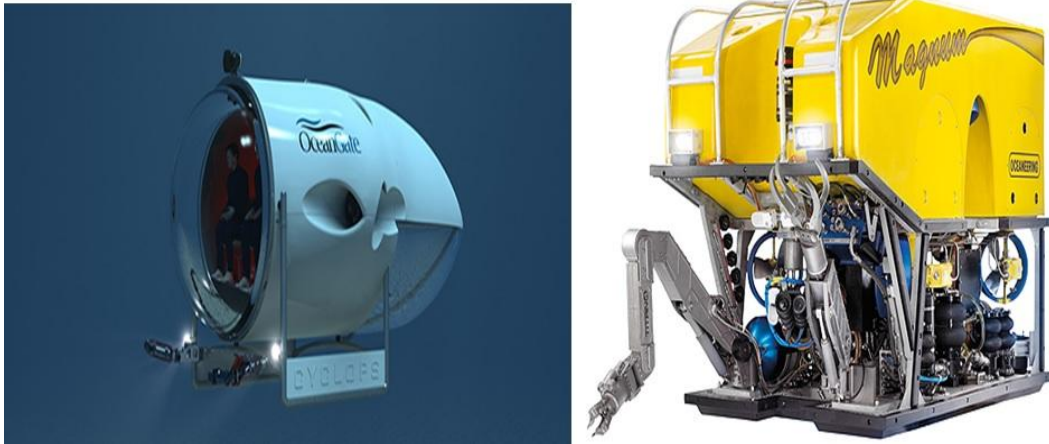


Fig 1.4:HOV Alvin and ROVs Janson used for deep see exploration. Photo courtesy (NOAA)

b) Thermal insulation:

The incorporation of HGM in syntactic foams produces 30-50 vol% voids in syntactic foams. The uniformly distributed voids pockets and insulating nature of epoxy matrix provide insulating properties to syntactic foams. These materials provide insulation for deep sea oil and gas pipelines. External fuel tanks used in space vehicles are also made of syntactic foams which provide thermal insulation in space.

c) Dimensional stability and low coefficient of thermal expansion:

Syntactic foams are used as composite material tooling boards and plug assists because of their high thermal stability and low CTE. Low CTE of tooling leads to only small dimensional changes and distortions as the temperature changes during composite fabrication for reason such as exothermic curing temperature. The Air Force Research Laboratory (AFRL) reported the use of carbon nanofibres and other nanomaterial-reinforced syntactic foams for space mirrors [37]. Low CTE of syntactic foams has been useful in developing space mirrors that maintain dimensional stability during rapid and large temperature changes. [38]

1.4. Aims and Objectives

This project deals with a novel approach to fabricate syntactic foams using nanofibres as reinforcement. The effect of adding nanofibres on the compressive properties of syntactic foam is an interesting area of research and therefore motivated us to carry this work. The reason behind the improved mechanical properties of foamed composites when adding nanofibres is the arrest of a crack front upon encounter of nanofibre. Light weight functionality of nanofibre leads to enhancement of overall strength without increase in weight and which is the ultimate aim of this report.

A systematic methodology highlighting the progress of the proposed work involves following steps:

- Preparation of polymer nanofibers by optimizing various parameters.
- Scanning electron microscopy of the nanofibers to obtain fiber size distribution
- Studying the effect of concentration on the fiber morphology via SEM studies
- Adding polystyrene and nylon 6 nanofiber separately in epoxy glass microsphere syntactic foam at varying volume fractions of fibre and micro balloons
- Adding nylon 6 nanofibre web as a sandwich layer in glass microsphere syntactic foam
- Quasi- static testing of the foamed composites which includes compression tests and flexural tests.

CHAPTER 2: EXPERIMENTAL

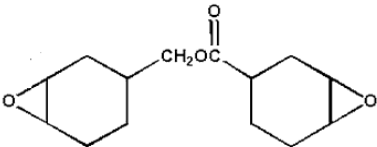

2.1. Introduction

This section deals with the preparation and characterization of nanofibers, their incorporation into the epoxy matrix at different volume fractions followed by preparation of syntactic foams.

2.2. Materials

Cycloaliphatic epoxy resin (Ciba Geigy, Araldite CY 230; epoxy equivalent 200 eq g⁻¹), hardener (HY 951; amine content 24 eq kg⁻¹) and Hollow glass microballoons (HGM, K15, 3M) were used as materials for preparation of syntactic foam. Polystyrene (GPPS), Dimethylformamide (DMF), Nylon 6 (Sigma Aldrich), Formic acid. The microballoons were kindly supplied by Chemtech Specialty, Mumbai. Double distilled water was used during the course of study.

Table 2.1: Properties of epoxy and TETA

Grade	Structure	Epoxy equivalent
CY 230		200 eq/g
HY951		Amine equivalent 32 eq/kg

2.3. Electrospinning set up

The entire equipment consists of the following parts:-

Spinning units including

- a. Spinning Chamber
- b. Syringe pump
- c. Drum / Disc/Plate collector
- d. Translation stage –for syringe pump
- e. Translation stage – distance between collector and syringe.
- f. Shorting stick

Control unit

- a. HV Power supply control
- b. Syringe pump control
- c. Drum collector control
- d. Syringe translation stage control
- e. Plate translation stage control
- f. Distance adjustment control



Fig 2.1: Setup of an electrospinning unit (ESPIN-NANO (PHYSICS EQUIPMENTS CO.)

2.4. Preparation of polystyrene nanofibers

Polystyrene nanofibers of different concentration and at different flow rates were prepared by electrospinning technique. For this purpose, homogeneous polymer solutions were prepared by dissolving 5 % (w/v) upto 20 % (w/v) polystyrene in DMF solvent at room temperature. Atleast 3, 2 ml hypodermic syringes were taken and they were filled with polymer solution. These syringes were then placed horizontally onto the syringe holder and were connected to wires for providing a potential gradient across the tip or the needle of the syringes to the collector. The collector used in the present study is a plate collector meant for collecting unaligned or random fibers. The collector was enveloped with aluminum foil on the side facing the needle for the ease of taking out the formed nanofibres from the plate. Once this set up was completed, the electrospinning assembly was closed and the flow rate was attuned from 0.1 ml/h to 5 ml/h as per the requirement. The space between the needle and collector was maintained at 14 cm. Finally a potential of 20,000 V was applied between the two ends. The polymer drops oozing out of the needles transformed themselves into cone shaped that eventually resulted in the generation of a charged jet of polymer solution that formed into fibers that travelled all the way to the collector. The polymer jet experienced bending and whipping instabilities and the jet path was chaotic. The randomly oriented non-woven nanofibers web obtained on the collector were removed with utmost care by turning the voltage to zero and complete switching off the setup followed by the use of a discharging stick to ground any residual charge that remained on the needles. Complete care was taken not to use bare hands prior to discharging and not to disturb the machine while operating. The samples were collected and subjected to analysis under SEM.

2.5. Preparation of nylon 6 nanofibers

Nylon 6 nanofibres were prepared by electrospinning similar to the one used for polystyrene. Nylon 6 was dissolved in formic acid at 10, 15 and 20 percent concentration (w/v). The solution so formed was transferred to syringes and placed onto syringe holder attached to syringe pump. Electric field of 20,000V and tip to collector distance 14 cm transformed the solution into fibres which was collected on aluminium foil at the collector.

2.6. Fabrication of neat and nanofiber reinforced syntactic foam

2.6.1. Fabrication of neat syntactic foam

Neat syntactic foams were prepared first by adding 40, 50 and 60 volume fractions of HGM respectively in epoxy matrix. The contents were mixed thoroughly and degassed to remove entrapped voids. Next 13 phr hardener was added to the above formulation and the resulting composition was transferred to silicone mould. The samples were cured at room temperature for 24 hours.

2.6.2. Fabrication of nanofiber reinforced syntactic foam

2.6.2.1. By random reinforcement

Different kinds of syntactic foams were fabricated, and the detailed compositions as well as sample designation are presented in **Table 2.2**. **SF** stands for syntactic foams, the polymer type is shown by "PS" or "N", which stand for polystyrene and nylon 6 respectively. The digits signify the volume fraction of HGM. For nanofiber reinforced foams, the last digits represent the volume fraction of nanofibres in the fabrication of syntactic foams (25 stands for 0.25% similarly 100, 200 and 400 stands for 1%, 2% and 4% respectively)

Polystyrene and nylon 6 nanofibres were randomly dispersed uniformly in epoxy resin through ultra-sonication for 30 min, following which glass microspheres were added. After thorough manual mixing, stoichiometric amount of hardener was added, mixed properly, and after degassing, allowed to cure in silicone molds for a period of 24 h at room temperature.

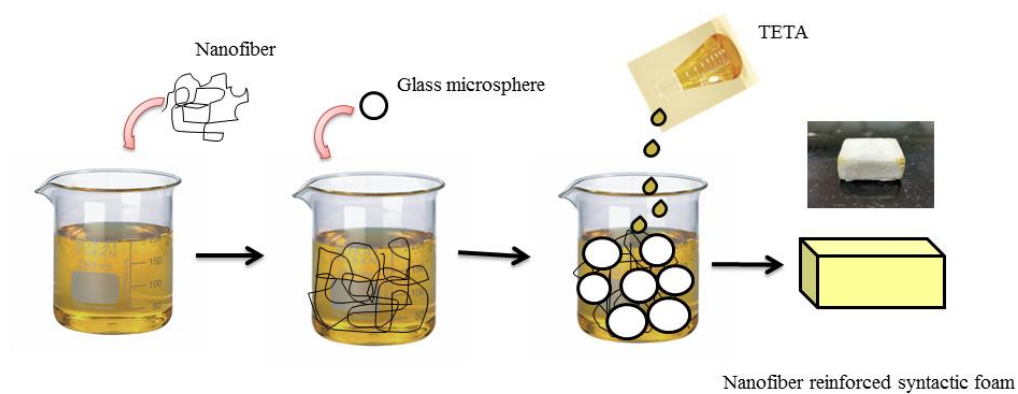


Fig 2.2: Steps for preparation of syntactic foam containing nanofibers

Table 2.2: Various compositions and designation of neat and nanofibers reinforced syntactic foam

<i>Sample Code</i>	<i>Matrix (% v/v)</i>	<i>Microballoons(% v/v)</i>	<i>Fibres(% v/v)</i>
SF40	60	40	-
SF50	50	50	-
SF60	40	60	-
SF40PS25	60	40	0.25
SF40PS100	59	40	1
SF40PS200	58	40	2
SF40PS400	56	40	4

SF40N25	60	40	0.25
SF40N100	59	40	1
SF40N200	58	40	2
SF40N400	56	40	4

The actual amount of HGM and fibre was calculated as per the formula

$$\frac{\text{Weight of fibre}}{\text{Weight of composite}} = \frac{\rho_{\text{fiber}} \times \Phi_{\text{fibre}}}{\rho_{\text{fiber}} \times \Phi_{\text{fibre}} + \rho_{\text{HGM}} \times \Phi_{\text{HGM}} + \rho_{\text{matrix}} \times \Phi_{\text{matrix}}}$$

The same formula was used for calculating the weight of HGM

2.6.2.2. Oriented reinforcement

The influence of fiber arrangement on the mechanical properties of syntactic foam was also of interest. For this purpose, epoxy, cenospheres and hardener was first mixed thoroughly and degassed prior to transferring to silicone moulds. Nanofibrous web of nylon 6 (0.25%) was introduced along the horizontal axis as sandwiched layers to result in a layered structure as shown in the figure below.

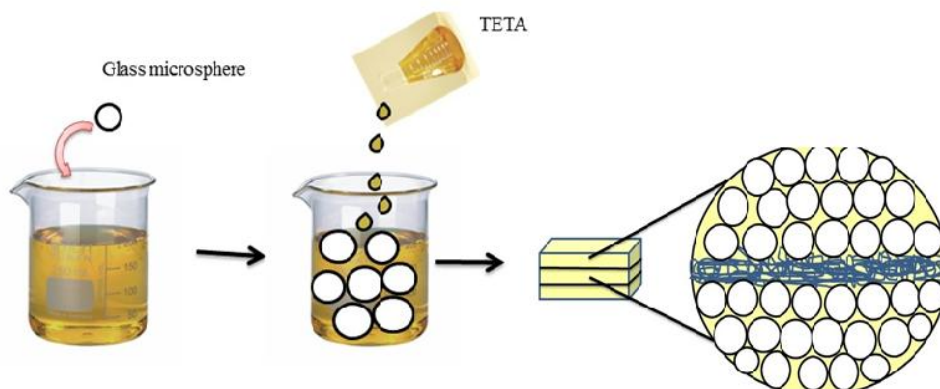


Fig 2.3: Layered nanofibre reinforced syntactic foam specimen

The samples were left for 24 hours for curing to take place. The specimen dimensions for compressive testing was 25mm × 25mm × 12.5mm and all testing was done in triplicate.

2.7. Density Determination

Theoretical density of syntactic foam (ρ_{th}) was calculated using the standard rule of mixtures.

$$(\rho)_{th} = (\rho)_{fiber} * (\Phi)_{fiber} + (\rho)_{HGM} * (\Phi)_{HGM} + (\rho)_{matrix} * (\Phi)_{matrix}$$

Here, ρ and ϕ represent density and volume fraction respectively. For calculation purposes, ρ_{fiber} (PS) and ρ_{fiber} (Nylon) has been presumed to be 1.05 g/cc and 1.14 g/cc respectively. The density of HGM has been reported to be 0.15g/cc. The density of epoxy was experimentally determined to be 1.49 g/cc.

2.8. Void volume

The theoretical density ($\rho)_{th}$ and experimental density ($\rho)_{exp}$ values are compared and the air void fraction trapped in the matrix during fabrication was calculated as per the following equation:

$$Void\ volume\ \% = \frac{\rho_{th} - \rho_{ex}}{\rho_{th}} \times 100$$

Experimental density was calculated by dipping the samples in distilled water and noting the volume of water displaced. Density is the ratio of weight of the sample in air to the volume of water displaced.

2.9. Characterization of fibres

2.9.1. Structural characterization

2.9.1.1 Scanning Electron Microscopy

The surface morphology of fibres was studied using a Scanning Electron Microscope (Zeiss EVO MA15) under an acceleration voltage of 20 kV. The morphology of the polystyrene

nanofibre, nylon6 nanofibre, fibre reinforced syntactic foam and compressed samples were carefully examined which were mounted on aluminium stubs and sputter-coated with gold and palladium (10 nm) using a sputter coater (Quorum-SC7620) operating at 10-12 mA for 120 s.

Principle:

Accelerated electrons in SEM carry significant amounts of kinetic energy, and this energy is dissipated as a variety of signals produced by electron-sample interactions when the incident electrons are decelerated in the solid sample. These signals include secondary electrons (that produce SEM images), backscattered electrons (BSE), diffracted backscattered electrons (EBSD that are used to determine crystal structures and orientations of minerals), photons (characteristic X-rays that are used for elemental analysis and continuum X-rays), visible light (cathode luminescence--CL), and heat. Secondary electrons and backscattered electrons are commonly used for imaging samples: secondary electrons are most valuable for showing morphology and topography on samples and backscattered electrons are most valuable for illustrating contrasts in composition in multiphase samples (i.e. for rapid phase discrimination).

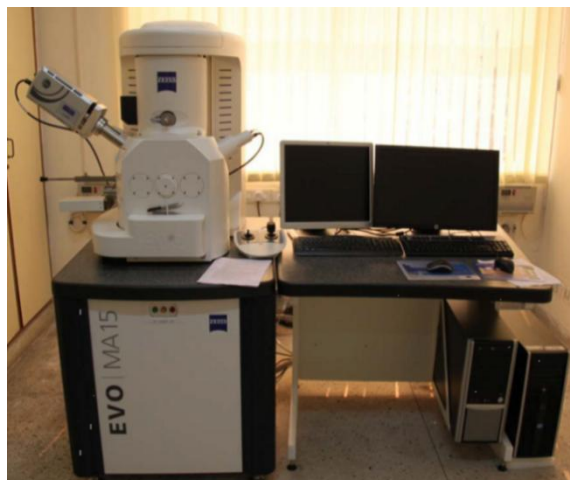


Fig 2.4: Scanning electron microscope

2.9.2. Thermal Characterization

2.9.2.1. Thermogravimetric Analysis

The thermal behaviour was investigated using Perkin Elmer Diamond STG-DTA under N₂ atmosphere (flow rate = 200 ml/min) in the temperature range 50-800 °C. A heating rate of 10 °C/min and sample mass of 5.0 ± 0.5 mg was used for each experiment.



Fig 2.5: Thermogravimetric analysis

Principal

Thermogravimetric analysis (TGA) is based on the measurement of mass loss of material as a function of temperature. In thermogravimetry a continuous graph of mass change against temperature is obtained when a substance is heated at a uniform rate or kept at constant temperature. The measurement is normally carried out in air or in an inert atmosphere, such as Helium or Argon, and the weight is recorded as a function of increasing temperature. A plot of mass change versus temperature (T) is referred to as the thermogravimetric curve (TG curve).

2.9.2.2. Differential Scanning Calorimetry

The changes in the thermal properties of the samples were investigated using DSC (TA instruments, Q 20 module) under nitrogen atmosphere. Approximately 4-6 mg of the sample was placed in a 40 μ L aluminium cap without pin and sealed with a lid. After erasing the thermal history of samples, they were subjected to a controlled heating program at 10 $^{\circ}$ C min⁻¹. Percentage crystallinity was calculated from the DSC traces as follows.

$$\%Crystallinity = \frac{\Delta H_{f, (observed)}}{\Delta H_{f, (100\% crystalline)}} \times 100$$

Where, $\Delta H_{f(observed)}$ is the enthalpy associated with melting of the material and $\Delta H_{f(100\% crystalline)}$ is the enthalpy of 100 % crystalline material which is 2.30 J/g

2.10. Mechanical Testing

2.10.1. Compression Testing

Compression test of the syntactic foams were done using a universal testing machine and it is used to signify how a product or material reacts when it is compressed, squashed, crushed or flattened by measuring fundamental parameters that determine the specimen behaviour under a compressive load. These include the elastic limit, which for "Hookean" materials is approximately equal to the proportional limit, and also known as yield point or yield strength, Young's Modulus (these, although mostly associated with tensile testing, may have compressive analogues) and compressive strength.

Compression testing provides data on the integrity and safety of materials, components and products, helping manufacturers ensure that their finished products are fit-for-purpose and manufactured to the highest quality.



Fig 2.6: Universal Testing Machine (UTM)

Principle

Certain materials subjected to a compressive force show initially a linear relationship between stress and strain. This is the physical manifestation of Hooke's Law, which states:

$$E = \text{Stress (s)} / \text{Strain (e)}$$

E is known as Young's Modulus for compression. This value represents how much the material will deform under applied compressive loading before plastic deformation occurs. A material's ability to return to its original shape after deformation has occurred is referred to as its elasticity. Vulcanized rubber, for instance, is said to be very elastic, as it will revert back to its original shape after considerable compressive force has been applied.

Once a certain force or stress threshold has been achieved, permanent or plastic deformation will occur and is shown on graphs as the point where linear behaviour stops. This threshold is known as the proportional limit and the force at which the material begins exhibiting this behavior is called the yield point or yield strength. A specimen will then exhibit one of two types of behavior; it will either continue to deform until it eventually breaks, or it will distort until flat. In either case a maximum stress or force will be evident, providing its ultimate compressive strength value. Compressive testing is an important test for syntactic foams a typical curve is obtained. The curve is divided into two sections mainly, the rise section and a plateau region, the rise section tells us about the linear rise of strain with stress but the plateau region or the densification region signals the breaking of the micro balloons under compressive loading. The micro capsules break resulting in the exposure of the inner surface to the compressive load and thus absorb sufficient stress in this process. The compression testing of the samples were carried out under a uniform strain rate of 1.33 mm/min

2.10.1.1. Compression testing of fibers reinforced syntactic foam

2.10.1.1.1. Polystyrene nanofibers syntactic foam

Samples (25mm × 25mm × 12.5mm) were prepared and tested as per ASTM (C365-94) standard [38]. At least 3 specimen of each type of reinforced syntactic foams were tested under a constant compression rate of 1.3 mm/min. Load displacement data was calculated in the tests and then transformed to stress-strain information in order to calculate compressive strength and modulus of polystyrene nanofibers syntactic foams. The area under the stress strain curve was calculated, which has been stated as the energy absorption of the foams.

2.10.1.1.2. Nylon6 nanofibre syntactic foam

Samples containing different fibre arrangements, as shown in figure 2.7 (a) and (b) were considered for compression testing. In one of the specimens,

the XY fibers plane was perpendicular to the load axis as shown in Fig. 2.7 (a), while in the other; the XY plane was parallel to the load axis as shown in Fig. 2.7 (b). Testing of random reinforced syntactic foam was also performed under similar conditions.

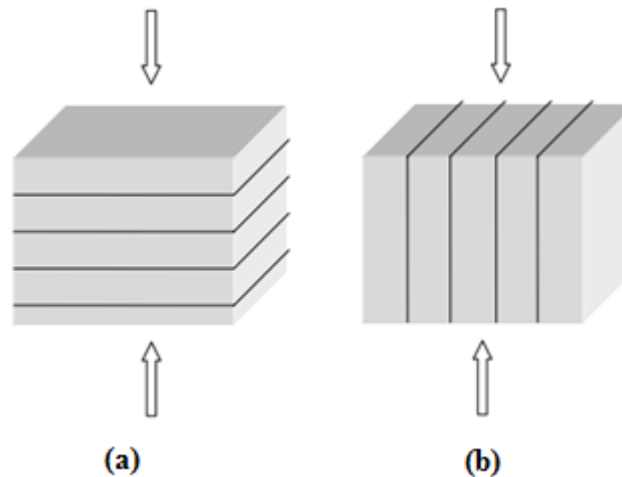


Fig 2.7: Arrows shows the loading direction and black lines specify the preferred orientation of fibers

2.10.1.2. Energy Absorption Mechanism in syntactic foam

The energy absorption features of syntactic foam materials render them interesting candidature for applications where protection against blast and/or impact is required. Figure 2.8 shows a typical quasi-static compression stress-strain response of a syntactic foams material.

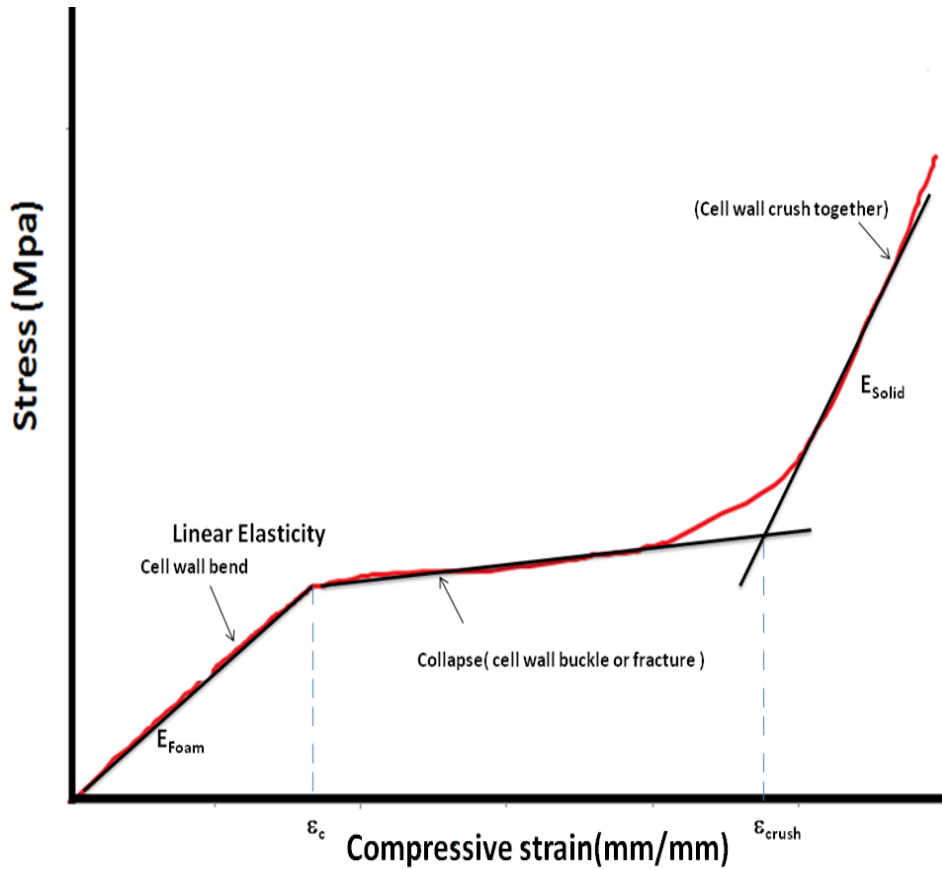


Figure 2.8: Compression stress-strain response of syntactic foam

E_{foam} is the ratio of σ_c and ϵ_c . The area under the stress-strain curve is representative of the toughness of the material. When the foam cell walls collapse, the modulus of the solid material is referred to as E_{solid} , which has no role to perform in the energy absorption mechanism. The energy absorption of foams can be compared by quantifying the area under the stress strain curve as follows:

$$Energy\ absorption = \frac{1}{2} (\rho_c \times \epsilon_c) + (\rho_c \times \epsilon_{crush} h)$$

Where,

σ_c =compression strength

ϵ_c = failure strain

ϵ_{crush} =crushing strain

The first term is the strain energy of the foam at failure and the second term is the crushing energy.

2.10.1.3. Flexural testing

Flexural testing of the samples was performed under 3 point bending mode as per ASTM D790. For this purpose, specimens of relevant dimensions (127 mm length x 2.5 mm width x 3.5 mm thickness) were prepared and subjected to a deformation rate of 2 mm/min along with maintaining 60 mm span length. The samples were tested on Instron 3369 machine with a 50 kN load cell.

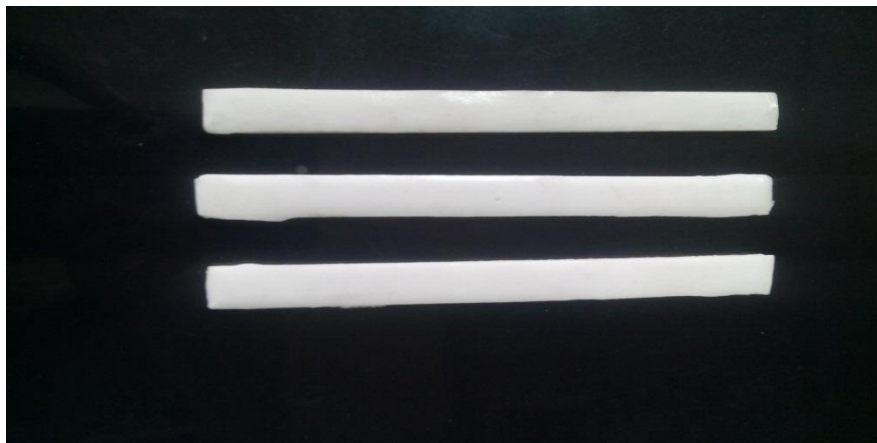


Fig 2.9: sample of flexural testing

CHAPTER 3

RESULTS AND DISCUSSION

3.1. Syntactic foams

Syntactic foams using epoxy as matrix and hollow glass microballoons(HGM) at different volume fraction (40%, 50%, and 60%) were prepared, the overall idea was to obtain reduction in weight without compromising the strength of foamed composite. This section discusses the fabrication of syntactic foams, both neat and fibre reinforced at varying volume fractions. The chapter is divided into two sub sections, the first part deals with the preparation and characterization of neat syntactic foams consisting of different volume fractions of HGM and the latter half of this chapter deals with the preparation and characterization of fibre reinforced syntactic foams.

Polymeric nanofibers have been chosen as suitable fillers in epoxy matrix, primarily because of their high surface area per unit weight that helps in obtaining substantial reduction in density of the foam compared to the conventional composites. Polystyrene and nylon 6 nanofibers have been added as reinforcements in syntactic foams separately. The effect of adding two different fibres on the mechanical properties of foams have also been studied in detail and results are presented in the following sections. Polystyrene was chosen in view of its higher modulus (3000 MPa) as compared to epoxy (818 MPa) [39]. Aramid fibres are a popular choice when it comes to using them as fillers in cenospheres filled composites[40]. The use of Kevlar fibres in enhancing the mechanical properties of composites encouraged us to take nylon 6 nanofibers as fillers in epoxy matrix glass cenospheres foams. The order of the results discussed here includes, the surface morphology of neat syntactic foam, effect of adding glass microballoons at different volume fractions on the mechanical properties, especially the compressive property of the foam, their thermal studies and fabrication of

fibre reinforced syntactic foam which in turn focuses on fibre formation via electrospinning , the effect of concentration on the morphology of nonwoven fibrous web and the fibre size distribution at different flow rates. After the fibres have been prepared, the incorporation of these electrospun fibres in the physical foams is depicted through scanning electron microscopy analysis; the effect of orientation of nylon 6 fibre on the flexural properties is represented in this report. Finally a conclusion is drawn from the results obtained so far.

3.2. Glass microballoons

The glass microballoons used in the present study, which are being increasingly used in many areas such as weight reduction, lower costs and enhanced product properties applications. They are chemically stable soda- lime-borosilicate glass and possess excellent water resistance, non-combustible and non-porous so that they don't absorb resin. The microballoons used are manufactured by 3M and kindly supplied by ChemtechSpeciality. Physical properties of these microballoons as supplied are presented in table below:

Table 3.1: Properties of Microballoons

Microballoons	Average true particle Density	Isostatic Crush	Thermal Conductivity
Type	(kg/m ³)	Strength (psi)	(W-M ⁻¹ K ⁻¹)at21° C
K15	150	300	0.055

3.3. Neat syntactic foam

Neat syntactic foam with different volume fractions of glass microballoons was prepared as described in the experimental section. SEM image of uncompressed foam shows the

presence of hollow glass balloons embedded in epoxy polymer matrix. The glass microballoons can be clearly observed as round particles. The debris shows some microballoons damage due to shearing during cutting of the samples.

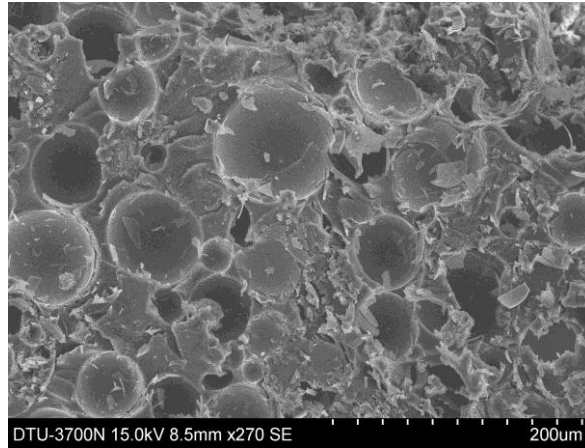


Fig 3.1:Representative image of neat syntactic foam

The effect of varying the volume fraction on the mechanical properties is highlighted below:

3.4.Mechanical Testing

3.4.1. Compression Test

Compressive strength and modulus of neat syntactic foam at strain rates of 1.33 mm/min were calculated from the stress strain curve of syntactic foams as shown in figure below:

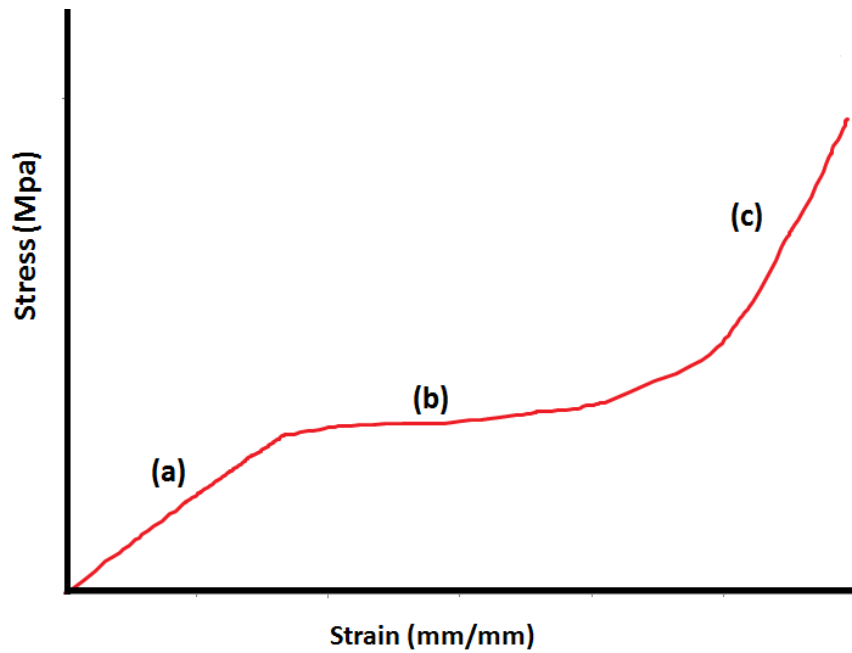


Fig 3.2: Representative stress strain curve of syntactic foam

The compressive stress strain curve of syntactic foams is shown above and consists of 3 regions denoted by ‘a’, ‘b’ and ‘c’ which correspond to elastic region, plateau region or densification region and end of densification region respectively.

It is evident from the stress-strain graph of syntactic foams that there is a gradual increase in strain as the stress increases. This is the initial region of the stress strain curve, marked as ‘a’ and is known as the elastic region or the Hookean region. The initial straight line graph rises to a maximum and then drops onwards; the region where the stress attains a maximum value is the peak value of the graph in the elastic region. This is also called as the yield point and the stress at this point denote the yield stress. Beyond the elastic zone, there is a drop in the stress value and the graph enters a plastic region which is characterized by linear increase in strain without a prominent increase in strain. At this region, the strain increases but the stress values remain fairly constant. The region where stress remains constant is called as plateau region or the densification region, marked as ‘b’. This section of the graph is a characteristic feature of foams. The reason for such behaviour of the stress strain curve can be understood

as, when a material, basically foam is loaded in a compression test, the hollow vacancies inside the matrix, absorb the pressure and prevent the stress levels from increasing. The same phenomenon happens in syntactic foams as well. Syntactic foams contain hollow glass micro balloons, these micro balloons when loaded tend to compress and beak so that they expose their inner surface to stress and in the process of doing so they absorb sufficient stress. The region denoted by 'c' on the above curve refers to the end of the densification region. After all the microspheres get crushed they cannot absorb the stress and eventually there a sudden rise in stress levels at a small strain and this marks the failure of the foam. The SEM image of the compressed foam in the plateau region is shown in fig. 3.4. The visual presence of HGM cannot be seen. The microballoons present in the specimen get crushed under heavy compressive loads. Once all the glass balloons get crushed, there is sudden increase in the stress and this marks the failure of the foam.

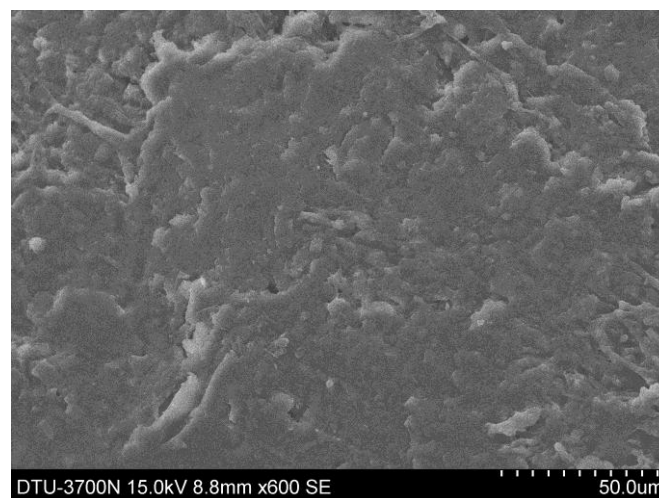


Fig 3.3: SEM image of compressed syntactic foam

3.4.1.1. Effect of volume fraction on compressive properties of syntactic foam

The compressive stress strain curve of neat syntactic foam obtained experimentally was very similar to the one shown above. For comparison purposes compressive stress strain curve of neat epoxy has also been added. Neat foams at different volume fractions were subjected to compression testing and graph obtained is shown in figure below.

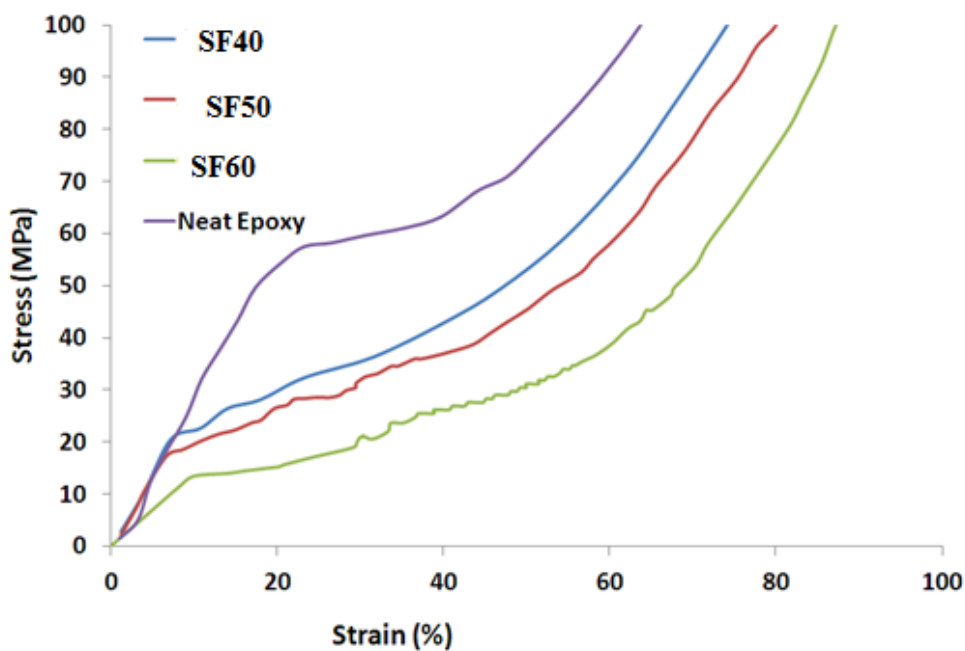


Fig 3.4: Compressive stress strain curve of neat syntactic foams containing varying HGM loadings

It can be inferred that as the volume fraction of glass micro balloons in syntactic foams increase, the strength decreases. This is pictorially presented in Figure 3.4. The decrease in strength can be attributed to the fact that at low volume fraction, there is sufficient matrix present to hold the cenospheres and the structure of the foam remains intact. But at higher volume fractions, there is an unavailability of matrix to bind the microspheres together and so at moderately low loads there is a collapse of the structure of the foam.

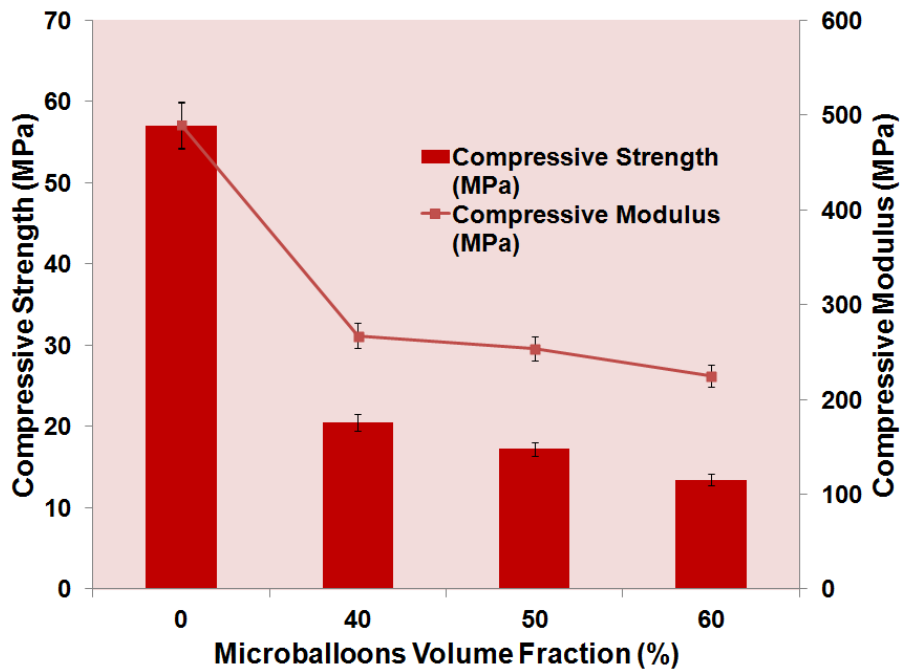


Fig 3.5: Comparison of compressive strength of neat syntactic foams at varying HGM volume fraction

3.5. Nanofibers reinforced syntactic foam

To enhance the mechanical properties of the foam, without increasing the weight further, we added nanofibers of polystyrene and nylon 6 which in turn were prepared by electrospinning route. As a representative scenario, nanofibers were added to formulations containing 40% HGM loading. This subsection focuses on the morphology of the fibres and the effect of flow rate and solution concentration on the fibre diameter.

3.5.1. Polystyrene nanofibers

Polystyrene nanofibers were electrospun at different flow rates and concentrations. The morphology of the spun fibers was examined using scanning electron microscopy.

3.5.1.1. Effect of Concentration on the polystyrene fibre morphology

SEM images of electrospun polystyrene nanofibres at varying concentrations (5-20) % (w/v) is presented in Figure 3.6 below . It can be seen that smooth bead free fibers could be obtained only at higher concentration of polymers used in electrospinning. As the polymer concentration increases, the viscosity of the solution increases, which lead to higher polymer chain entanglements and continuous fibers can be attained without breaking the jet of the solution throughout the electrospinning process. It is interesting to mention here that at 5 % (w/v) concentration, beads are obtained due to insufficient chain entanglements in the solution which is a result of low viscosity and high surface tension of the polymer drop. At concentrations of 10 and 15 percent (w/v), small size beaded fibres are obtained. Uniform bead free fibres are obtained at polymer concentrations of 20 % (w/v), however further increase in concentration is impractical in view of the extremely high viscosity of the solution.

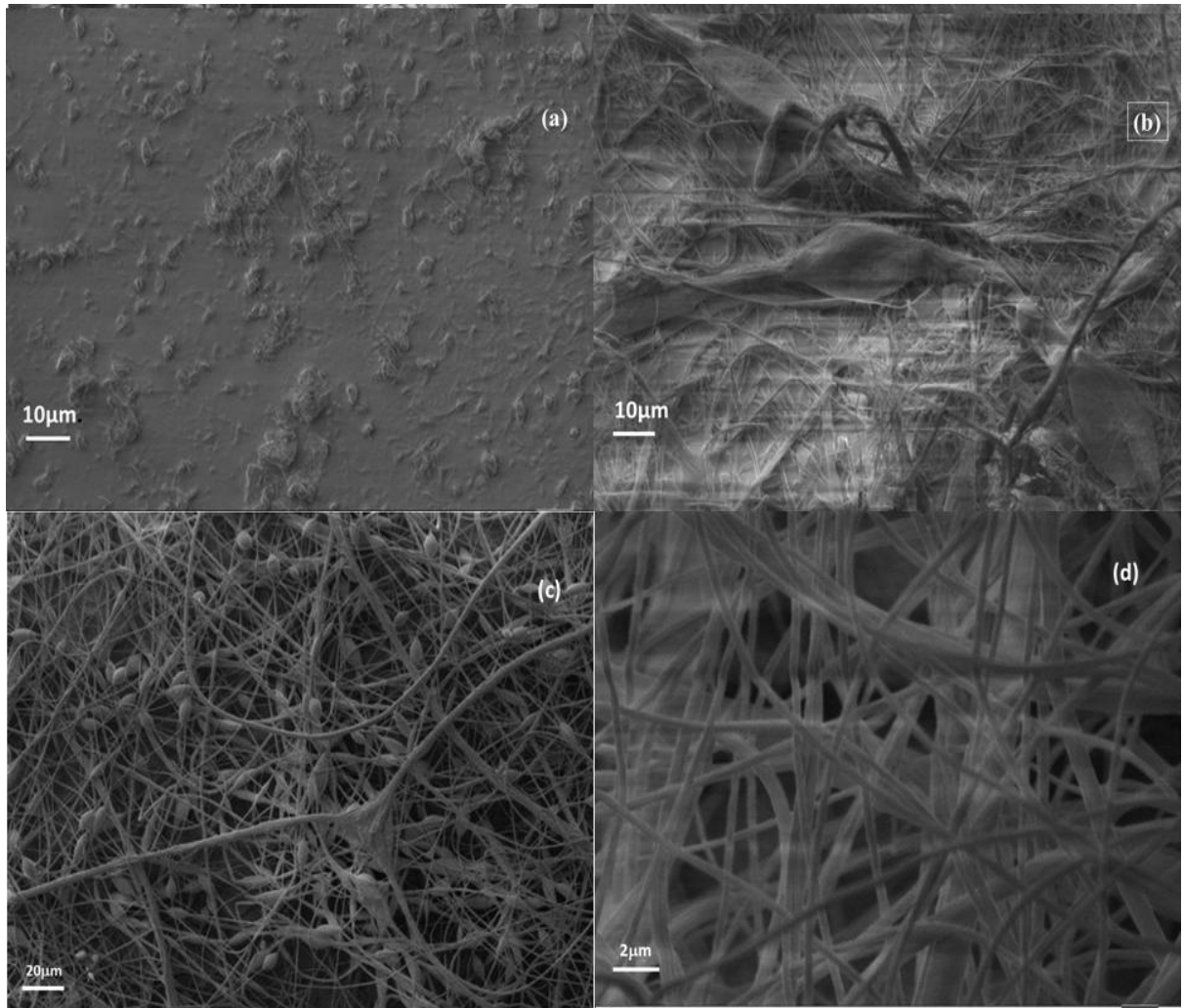


Fig 3.6: Effect of concentration on the surface morphology of polystyrene nanofibres at different concentrations: **(a)** 5% (w/v) **(b)** 10% (w/v) **(c)** 15% (w/v) **(d)** 20% (w/v)

3.5.1.2. Effect of flow rate on polystyrene nanofibers morphology

Flow rate also plays a crucial role in determining the fibers dimensions. At low flow rates of 0.1ml/h, the polymer drop emerging from the needle tip has sufficient time to undergo polarization, which in turn leads to splitting and results in fibers with significantly low diameter. As the flow rate was increased from 0.1ml/hr to 5ml/hr, the diameter of fibers increased, as can be seen in the SEM images (Figure 3.7)

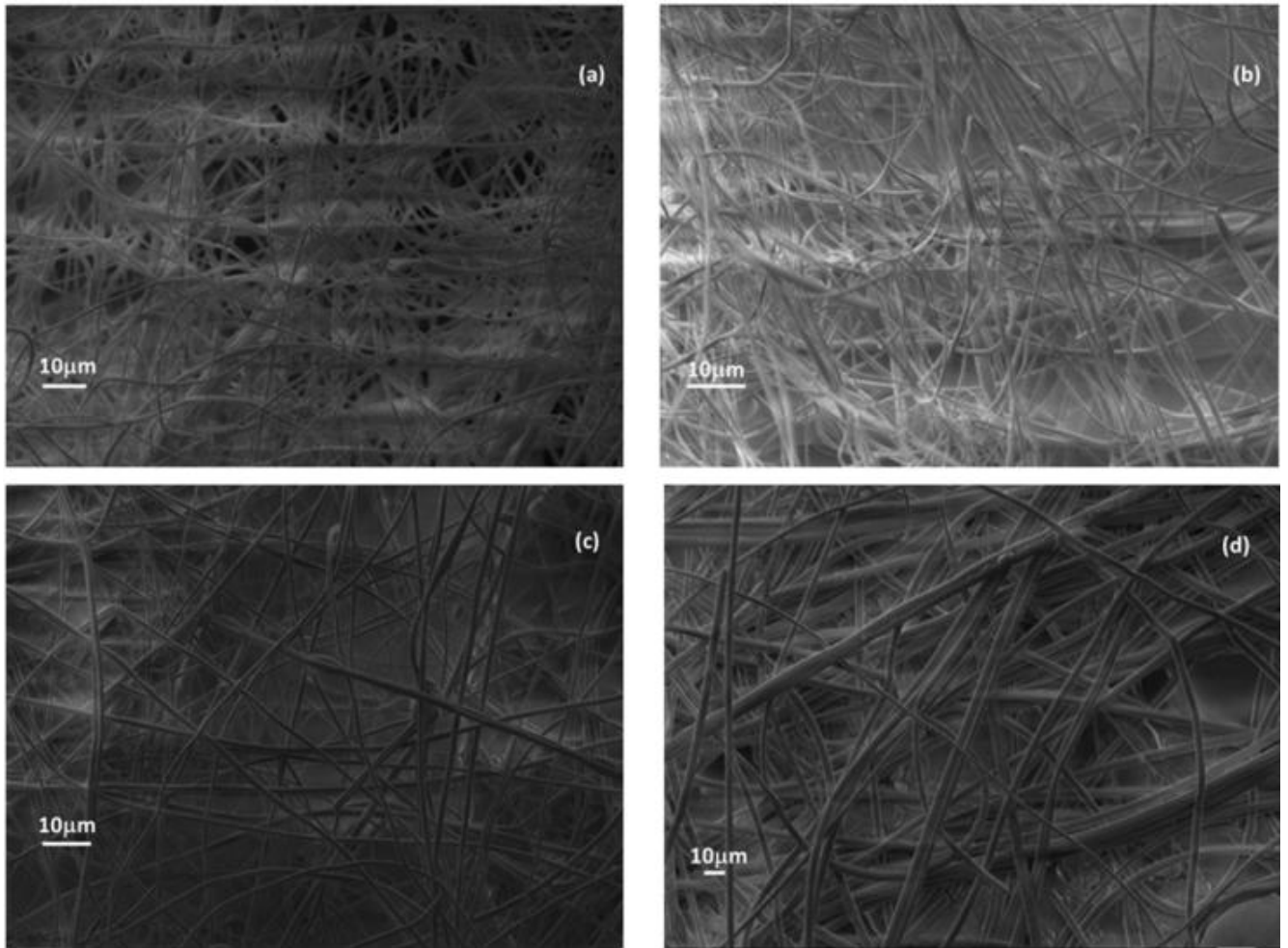


Fig 3.7: Effect of flow rate on surface morphology of polystyrene nanofibers at rates:

(a) 0.1ml/h, (c) 1ml/h, (d)3ml/h and (e) 5ml/h

3.5.1.3. Fibersize distribution

The effect of flow rate on the fiber size distribution is presented in Figure 3.8. The diameter of fiber was observed from the SEM images of electrospun PS fibers. As expected, increasing the flow rate led to a systematic shift in the distribution towards larger diameter.

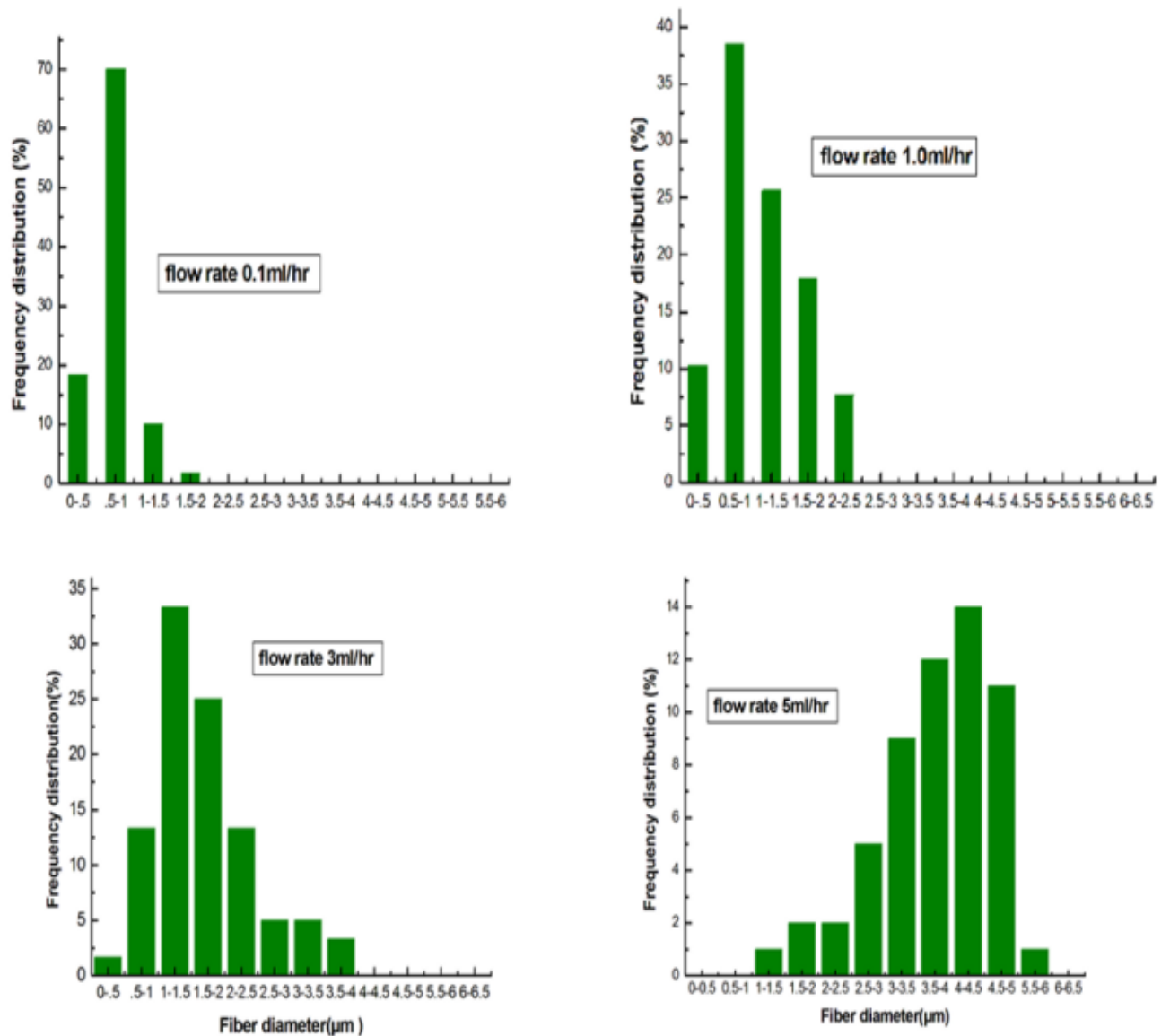


Fig 3.8:Fiber size distribution at flow rates (a) 0.1 ml/hr(b) 1 ml/hr(c) 3ml/hr(d) 5ml/hr

3.5.1.4. Thermal characterization

The thermal stability of the samples was studied using thermogravimetry. The TG-DTG trace of polystyrene fibers is presented in Figure 3.9. TGA trace depicts the residual weight or weight loss as a function of temperature which has been shown by the solid line. The DTG trace is represented by a dotted line, the derivative of the weight loss as a function of temperature. The advantage of the DTG trace is the step of decomposition which involves very small weight loss.

As can be seen from the curve, polystyrene exhibits single step degradation with a mass loss of ~98% at 500 °C.

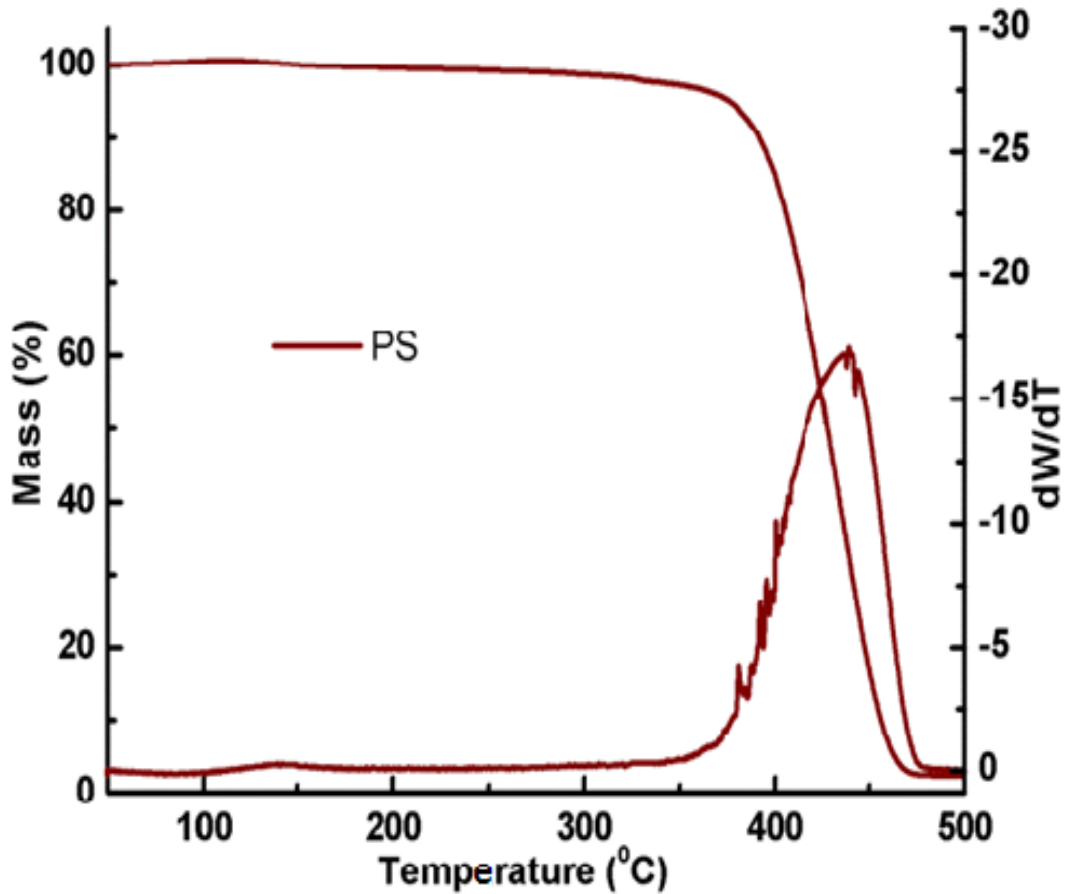


Fig 3.9: TG-DTG traces of polystyrene nanofibre

3.5.2. Nylon 6 nanofibre

Nylon 6 nanofibres were also prepared by electrospinning at different concentrations and flow rates. The effect of varying the concentration and flow rates is presented in the following sections.

3.5.2.1. Effect of Concentration on fibre morphology

Thin and smooth fibres were obtained at high concentration of nylon 6 solutions, the reasons for which have been discussed in previous section.

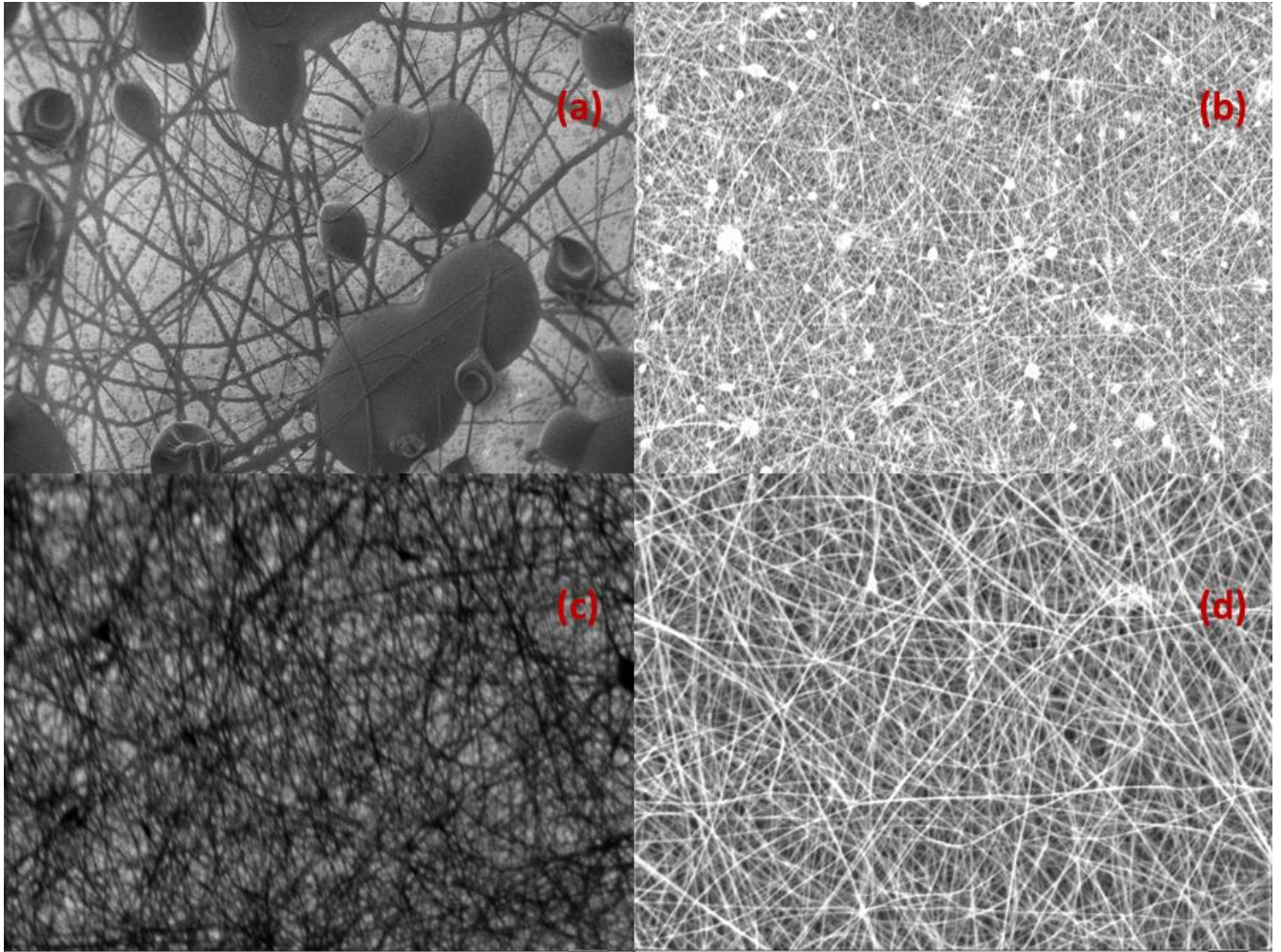


Fig 3.10: Effect of concentration on the surface morphology of nylon6 nanofibres at different concentrations: **(a)** 5% (w/v) **(b)** 10% (w/v) **(c)** 15% (w/v) **(d)** 20% (w/v)

3.5.2.2. Effect of flow rate on fibre morphology

An increase in flow rate resulted in increase in the thickness of fibres and the same is evident from the SEM images presented in Figure 3.11

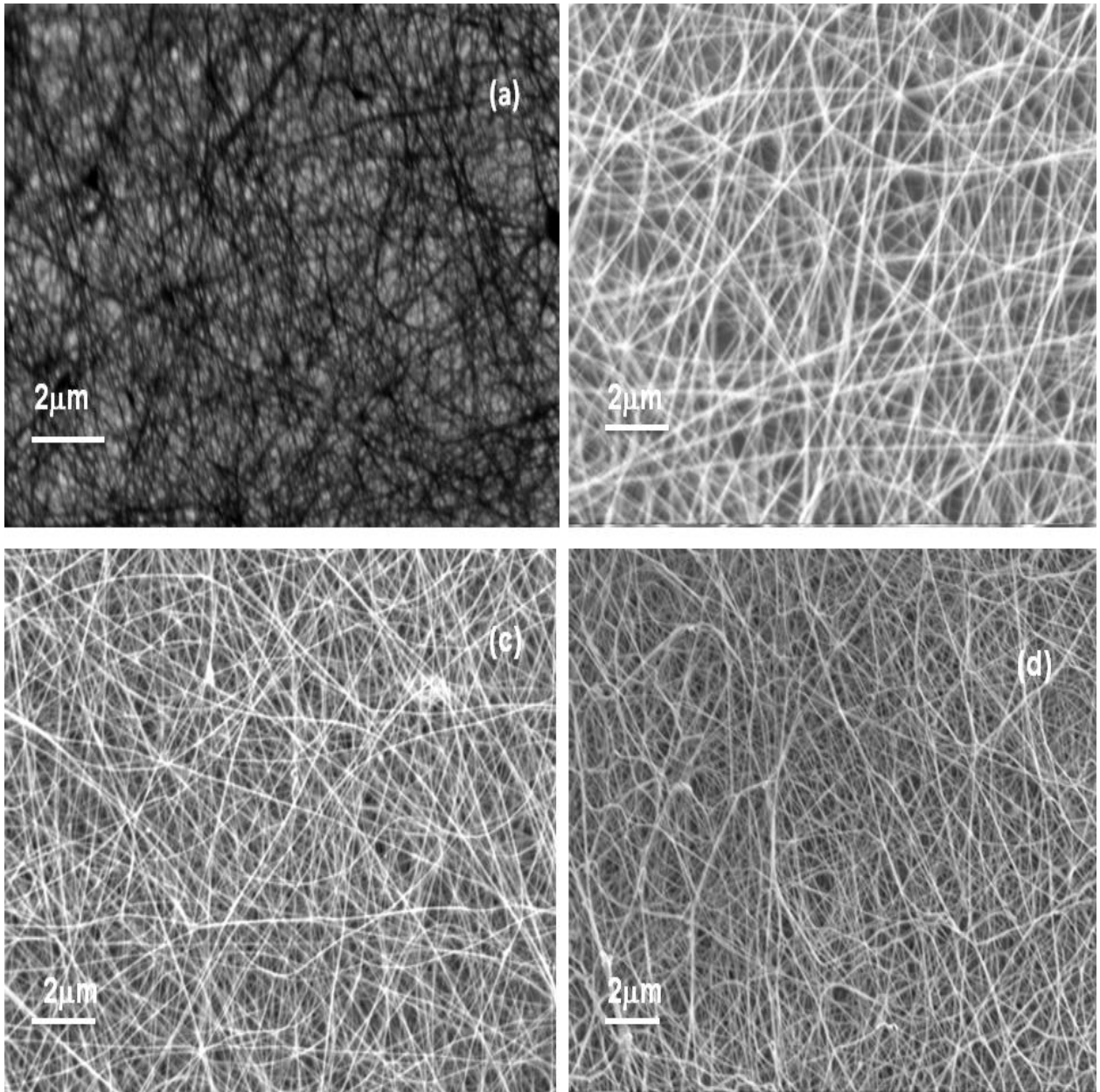


Fig 3.11: Effect of flow rate on surface morphology of nylon6 nanofibers at rates:

(a) 0.1ml/h, (b) 0.3ml/h, (c) 0.5ml/h and (d) 1ml/h

3.5.2.3. Fibersize distribution

The effect of flow rate on the fibersize distribution is presented in Figure 3.12. As expected, increasing the flow rate led to an increase in the fiber diameter.

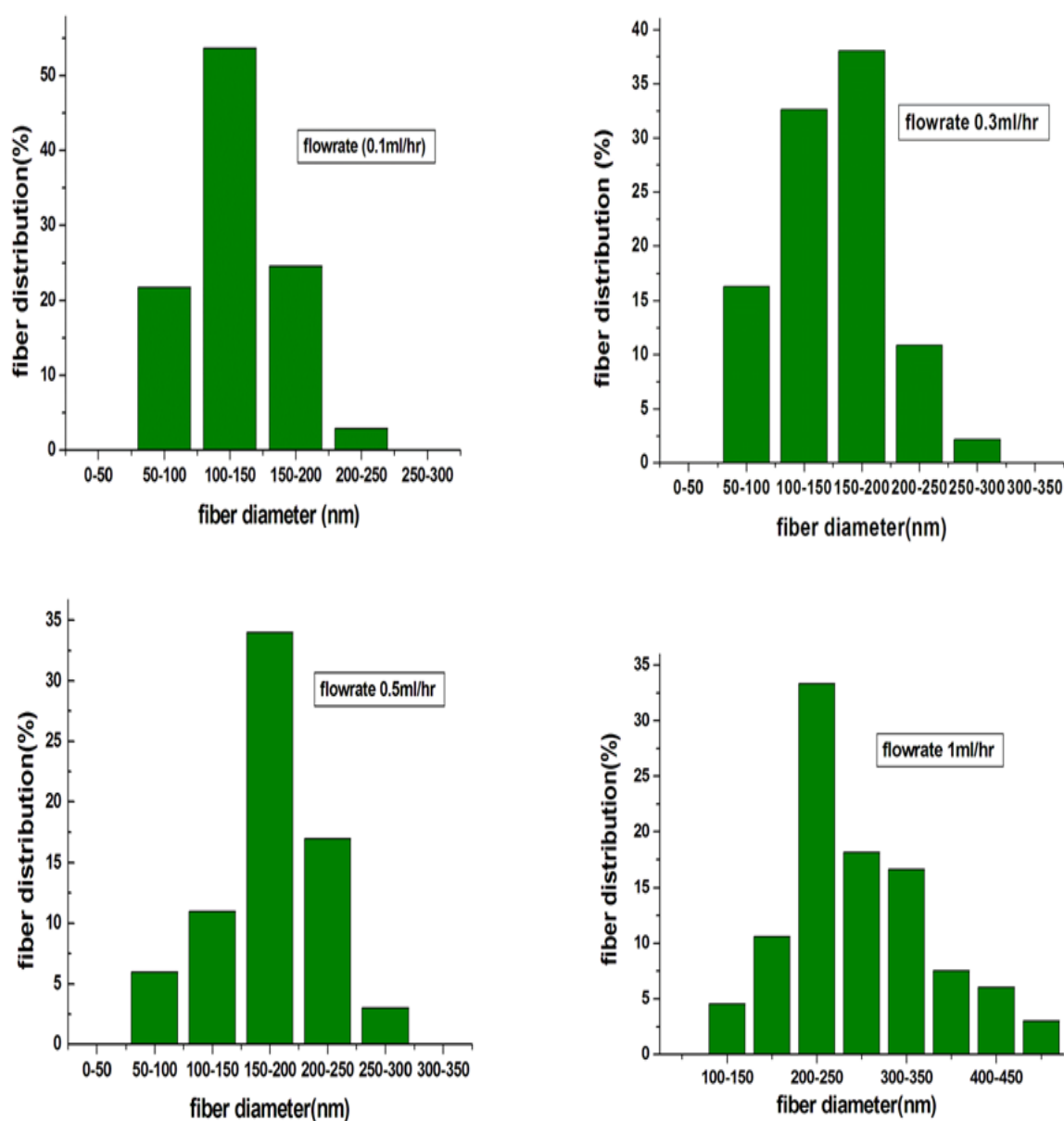


Fig 3.12: Fibre size distribution of nylon 6 nanofibers

3.5.2.4. Thermal Characterization

The TG-DTG and DSC traces of nylon 6 are shown in Figure 3.13-3.14. It can be seen that nylon is stable upto 200 °C. The maximum degradation takes place at 429.50 °C. A single step degradation pattern was observed in the TGA trace of nylon 6.

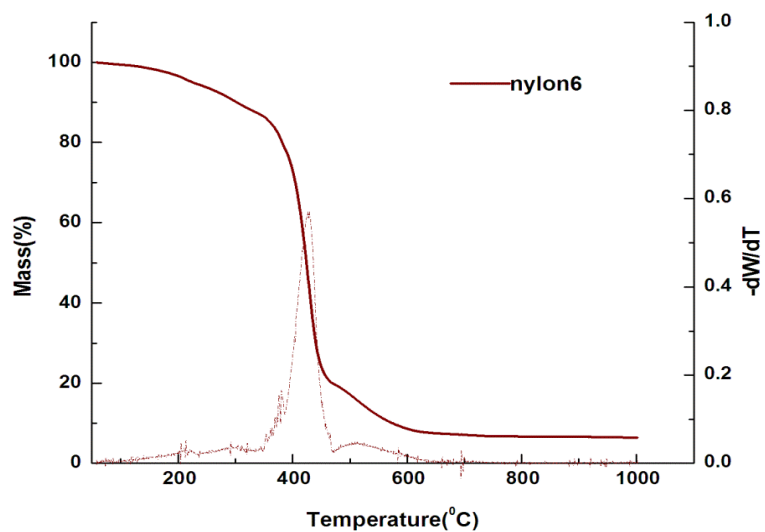


Fig 3.13: TGA-DTG of nylon6

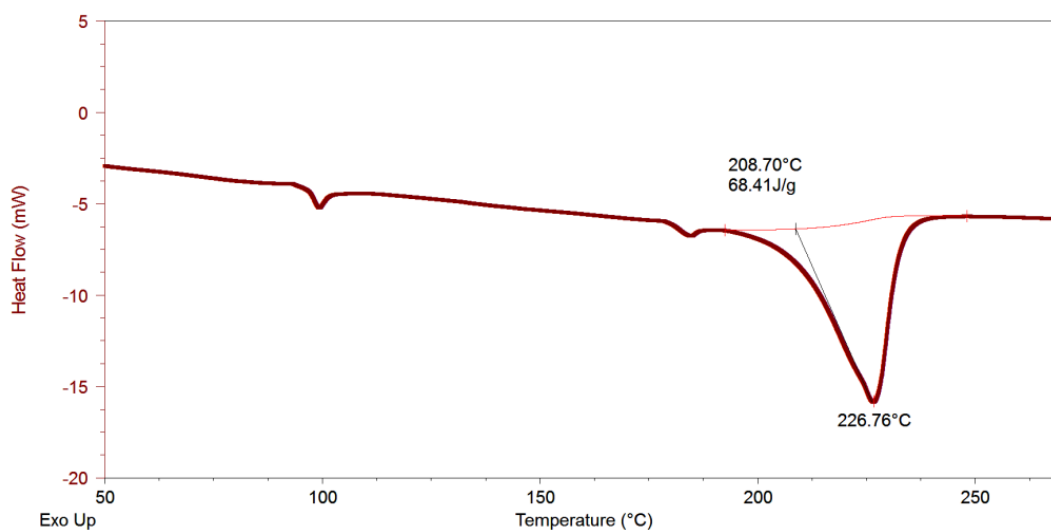


Fig 3.14: DSC trace of nylon 6 nanofibre

The DSC crystallinity of fibres was found to be 29 %, using $\Delta H_{100\% \text{ crystalline}}$ of 230 J/g

3.6. Nanofibres reinforcement in syntactic foams

Nanofibres of polystyrene and nylon 6 were introduced in syntactic foams at different volume fractions separately. The nanofibrous web was reinforced in glass microsphere syntactic foam

in different orientations. Two types of samples were prepared, which included random and oriented dispersion of the fibres.

3.6.1. Density Determination

The experimental and theoretical density of the syntactic foam compositions are presented in Table 3.2. The percentage of void as calculated from these is also presented.

Table 3.2: Experimental and theoretical density of neat and fibre reinforced syntactic foam

<i>Sample Code</i>	<i>Experimental Density (kg/m³)</i>	<i>Theoretical Density (kg/m³)</i>	<i>Voids (Vol %)</i>
SF40	904	954	5.2
SF50	770	820	6.0
SF60	686	716	4.1
SF40PS25	910	956	4.8
SF40PS100	923	949	2.7
SF40PS200	928	945	1.7
SF40PS400	901	936	3.7
SF40N25	930	953	2.1
SF40N100	946	950	0.4
SF40N200	943	947	0.4

3.6.2. Mechanical testing of nanofiber reinforced syntactic foam

3.6.2.1. Polystyrene nanofibre reinforced syntactic foam

3.6.2.1.1. Compression Testing

The effect of adding polystyrene nanofibres (0.25-4% v/v) in foams containing 40% v/v HGM was evaluated under compressive loadings and the results are presented in Figure 3.16 and Table 3.17. It can be seen that there is very little improvement in the compressive yield strength on adding nanofibres. The mechanism of energy absorption of foams is well reported in literature. Under the compressive loadings; the micro-spheres were crushed. The crushing of the microsphere left oversized voids and debris in the matrix, which lead to beginning of the crack. On compressive yielding, most of the microspheres were crushed and lead to severe damage. It appears that the failure of the specimen is dominated by the microspheres crushing, while nanofibres and the matrix play insignificant role. In other words, HGM is the primary load bearing phase in the hybrid syntactic foam when the specimen is subjected to compressive loading.

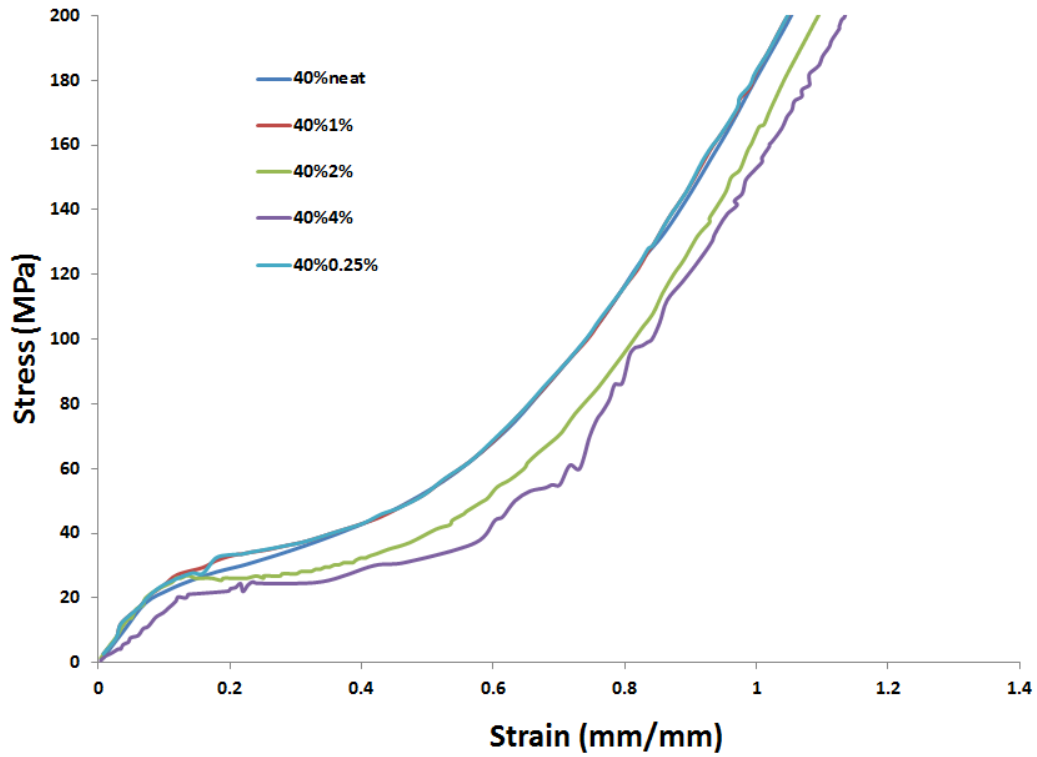


Fig 3.15: Compression stress strain curve of PSSF40 containing 0-4vol% PSNFs

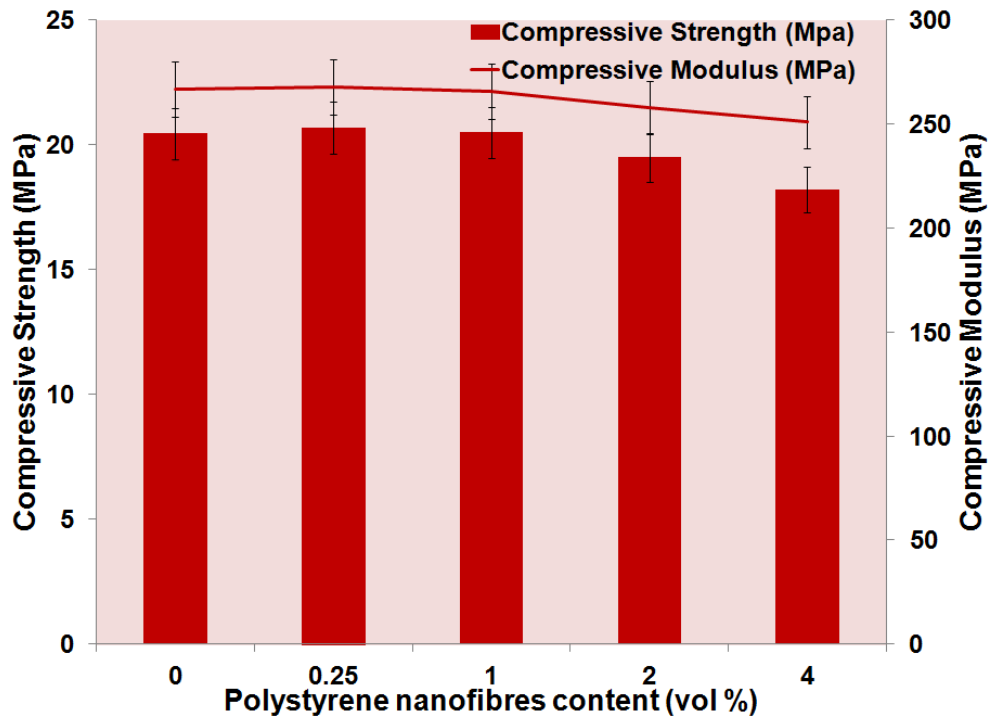


Fig 3.16: Comparison of compressive strength and modulus of SF40 at different nanofibre loadings

Hence, the presence of polystyrene nanofibres leads to small enhancement in the compressive strength of SF40 at 0.25 and 1 percent volume fractions.

3.6.2.2. Nylon 6 nanofibre reinforced syntactic foam

Addition of polystyrene led to only minor improvements in the compressive properties of syntactic foams at 0.25% volume fraction of fibres. For the purpose of toughening, the potential of polyamides fibers was also explored in view of the tough nature of Nylon 6. The presence of film can be seen in the SEM image, which is presented in Figure 3.17.



Fig 3.17:Fiber reinforced syntactic foam

3.6.2.2.1. Compression Testing

Compression tests were conducted on neat foam, random nanofibres reinforced syntactic foam and fibre reinforced foams in parallel as well as perpendicular direction of fibre axis and the influence of fibre arrangement was studied. The results obtained on addition of 0.25 volume percent nylon 6 in different orientations is presented in Figure 3.19 and Fig 3.20.

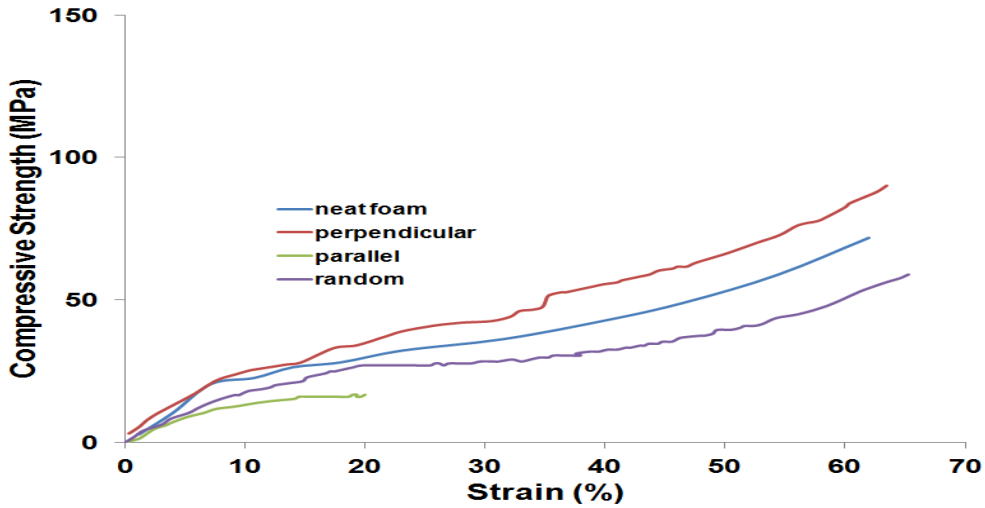


Fig 3.18: Compressive stress strain curve of SF40N25 at different orientations of nylon 6

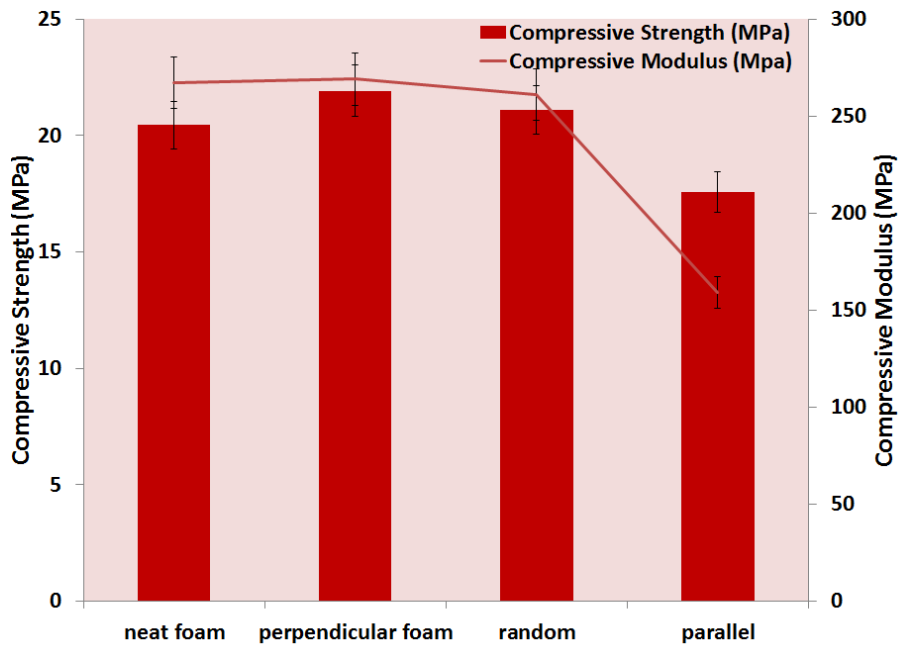


Fig 3.19: Compression strength and modulus of syntactic foams containing nylon 6

It is interesting to note the behaviour of foams containing nanofibres when tested under parallel mode compression testing with respect to nylon6 fiber axis, it is unable to withstand compressive stress as the de lamination of nylon6 plies take place due to the presence of voids in between the plies and epoxy hybrid syntactic foam



Fig 3.20: The photographs of compression tested samples (a) perpendicular, (b) parallel are presented (arrows indicate direction of loading)

3.6.2.2.2. Energy Absorption

Energy absorption parameter is calculated from the formula given in the experimental section. Toughness can be quantified as the energy absorbed per unit volume of syntactic foams. It is important to remember that the toughness of syntactic foams depends to a large extent on the crushing strain. Higher the length of the plateau region, higher would be the energy absorbed per unit volume. For nylon 6 reinforced syntactic foams, perpendicular conformation of nylon 6 plies absorbs sufficient amount of energy and thus shows remarkable improvement in toughness compared to neat foam. However, the toughness decreases on changing the arrangement of fibres suggesting that orientation of nanofibres has a larger role to play in enhancing the toughness of nanofibre reinforced syntactic foams. Figure 3.21 highlights the importance of fibre arrangement by means of a graph below.

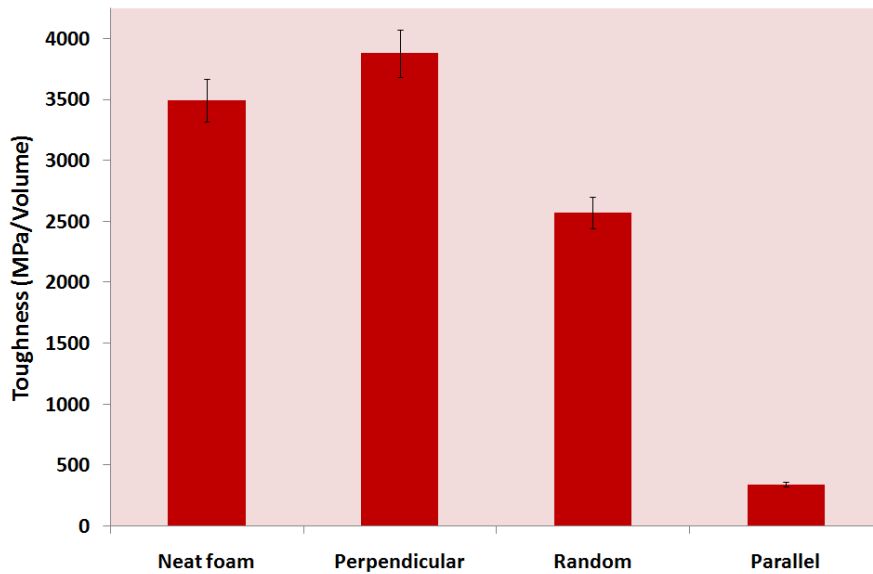


Fig 3.21: Influence of fiber arrangement on the toughness of SF40N25

3.6.2.2.3. Flexural Testing

Neat as well as nylon reinforced foams were subjected to flexural tests at a deformation of 2mm/min. Flexural strength was calculated from the stress strain curve and reported in Fig 3.22. In a flexural test, the sample undergoes compression on the top and tensile forces operate on the sides however the failure of the specimen under flexural mode is dominated by tensile mode which was evident from the debonding of microspheres.

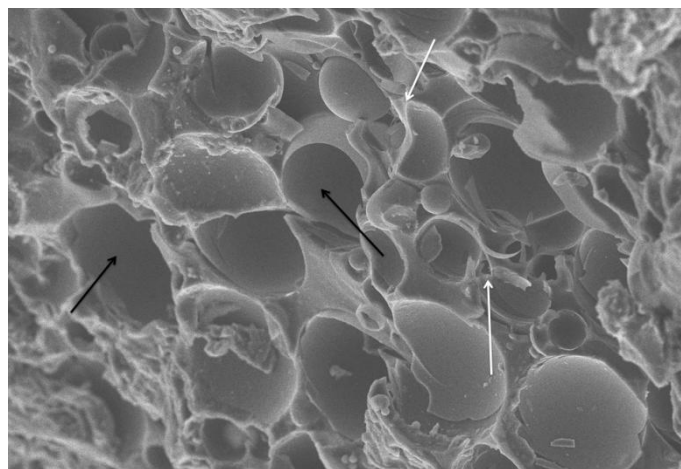


Fig3.22: SEM image of specimen after flexural test

It was noticed that the process under flexural loading involves debonding, fracture and deforming rather than crushing of the microspheres. Although deformed microspheres were present, their amount was much smaller than that of the debonded and fractured microspheres. The arrows in black indicate the presence of oversized voids due to debonding of microspheres whereas the white arrows indicate fracture of the microballoons under compressive loads. This is ascribed to the fact that the microspheres in SF40N25 are not the primary load bearing phase under flexural loading. The failure of the specimen is dominated by matrix fracture. This observation is distinct to the condition under compressive loading.

Table 3.3: Flexural strength and modulus of neat and nylon6 reinforced syntactic foam.

Sample	Flexural Strength (MPa)	Flexural Strain (%)	Flexural Modulus (MPa)
SF40	20	5.0	510.1
SF40N25	35	8.1	555.7

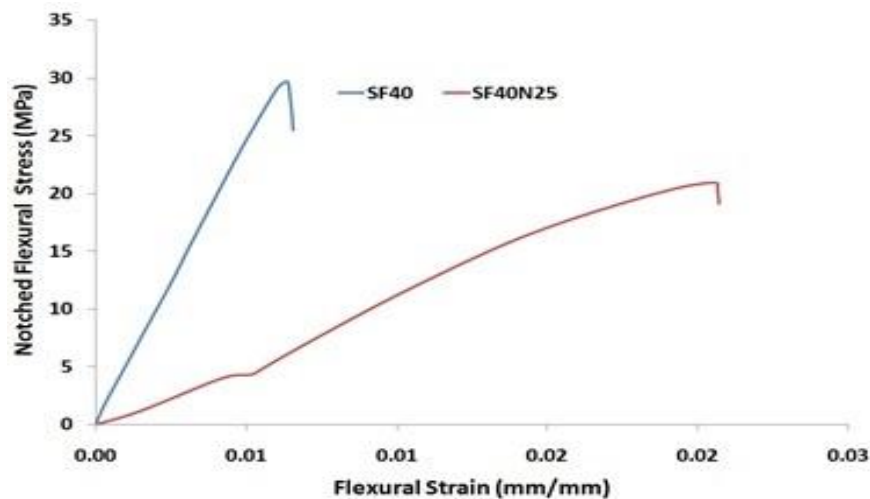
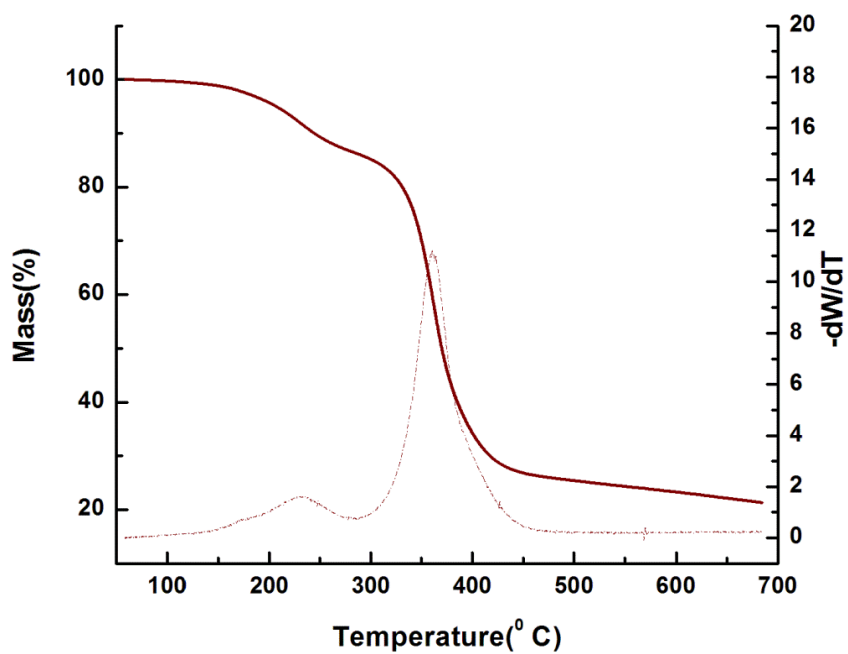
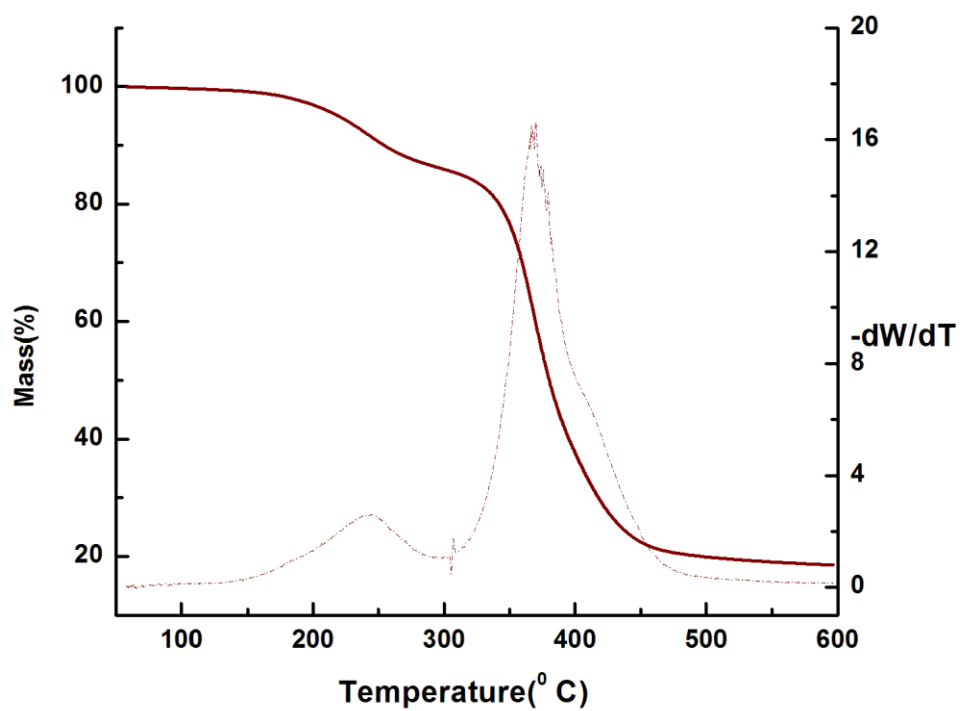


Fig 3.23: Flexural stress strain graph of SF40 and SF40N25

There was no improvement upon addition of nylon 6 nanofibres in syntactic foams because of poor interfacial adhesion between the film and the matrix which leads to the easy pull out of the fibrous film leading to generation of voids which are the weak links in providing the foams their strength.

3.7. Thermal Characterization of syntactic foam

TG and DTG traces of syntactic foam at different volume fractions are presented in Figure 3.24. A two stage degradation pattern can be seen in all the samples. The first step takes place at ~ 190 °C and is associated with the release of water and other condensable species



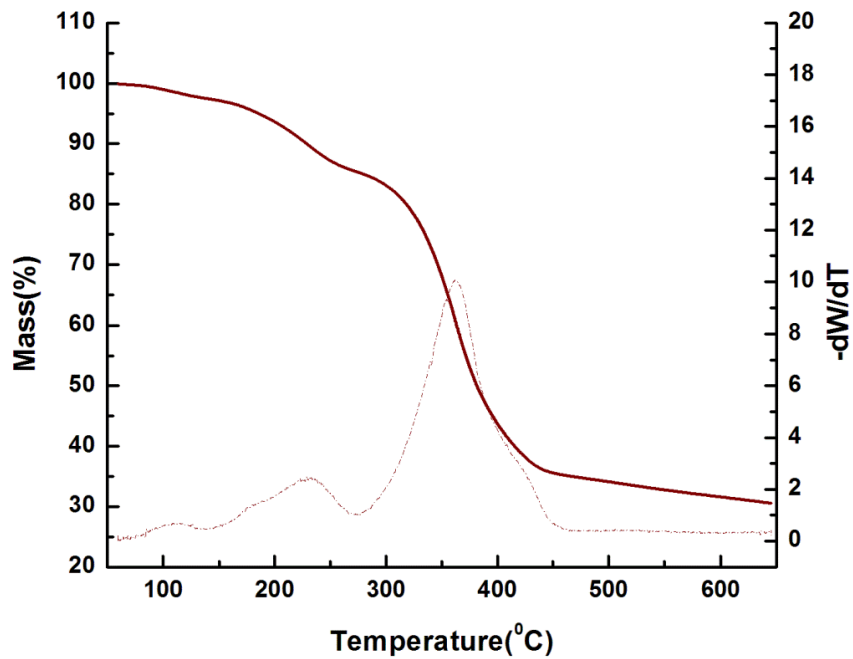


Fig 3.24: TGA and DTG traces of syntactic foams at different volume fractions (a) 40%, (b) 50%,(c) 60%. Solid lines represent TGA and dotted lines represent DTG traces

The thermal stability was compared by comparing the initial temperature of decomposition (T_{onset}), Final decomposition temperature (T_{end}) and temperature of maximum rate of weight loss (T_{max}) and the result are summarized in Table 3.4.

- I. **Initial decomposition temperature (T_{onset}):** The temperature at which the first weight loss was observed in the TG trace and was noted by extrapolation.
- II. **5% decomposition temperature ($T_{5\%}$):** The temperature at which 5 percent decomposition is observed in the TG trace.
- III. **Final decomposition temperature (T_{end}):** the temperature at which the weight loss virtually stops and is obtained by extrapolation of the final portion of TG trace.
- IV. **Temperature of maximum rate of weight loss (T_{max}):** Tmax was evaluated from the DTG traces .The temperature corresponding to the peak position of derivative plot was noted as Tmax.

Table 3.4: Characteristic decomposition temperatures of samples

<i>Sample</i>	$T_{(5\%)}$	$T_{(\text{onset } 1)}$	$T_{(\text{max } 1)}$	$T_{(\text{onset } 2)}$	$T_{(\text{max } 2)}$	$T_{(\text{end})}$	<i>Char</i>
<i>Designation</i>	(°C)	(°C)	(°C)	(°C)	(°C)	(°C)	<i>yield</i>
							(%)
Polystyrene	376.0	387.6	437.7	-	-	510.4	2
Nylon6	223.0	398.0	429.5	-	-		
SF40	218.6	191.8	239.4	346.4	368.7	591.1	18.5
SF50	201.7	201.7	230.2	336.3	360.7	638.1	22.4

CHAPTER 4

SUMMARY AND CONCLUSION

This project deals with the development of syntactic foams consisting of hollow glass microballoons filled in epoxy matrix with a primary aim of reducing the density without compromising on the strength. As expected, syntactic foams were much lighter than epoxy, but the strength was also substantially lowered. Electrospun nanofibres of polystyrene and nylon 6 were added in these materials to increase the load carrying capacity of such materials.

Polystyrene and nylon 6 nanofibre webs were prepared by electrospinning the polymers in suitable solvents. The operating parameters were optimized to obtain perfectly uniform and smooth fibres. Post electrospinning, the fibres were characterized by SEM imaging to determine their morphology and fibre diameter distribution.

Syntactic foams were prepared consisting of epoxy matrix and hollow glass cenospheres of K15. Some voids were also entrapped in the foams during their fabrication. Volume fraction of microballoons was varied (40-60 %). The prepared foams were subjected to compression testing at 1.33 mm/min deformation rate. Under compression load, the entrapped microballoons ruptured and crushed leading to the absorption of energy till a certain limit after which abrupt increase in stress was observed that resulted in the failure of foams. Compression strength was evaluated at different volume fractions; the results indicated higher compression strength at lesser volume fractions of HGM i.e. at 40 percent.

Nanofibres of polystyrene were added into the syntactic foams at 0.25, 1, 2 and 4 volume percent. Increase in compression strength and modulus was observed at 0.25 and 1 percent. Compressive strength was found to decrease at higher volume fractions which could be attributed to the agglomeration of nanofibres.

Nylon 6 nanofibres were reinforced at 0.25-4 percent volume fractions in specimens. Three different alignments of nylon 6 nanofibrewere tested, i.e. random, perpendicular and parallel with respect to the load axis. Compressive strength was highest for perpendicularly reinforced specimens followed by random and parallel orientations. However, the compression yield strength was lower in all cases when compared to neat foams but there was an improvement in modulus of perpendicular and random samples. Samples, where the load was applied parallel to the fiber axis, exhibited lowest strength and modulus.

Flexural testing of nylon 6 syntactic foams at 0.25 percent was also performed. However, no significant improvements in flexural strength, strain and modulus was observed, and all the samples exhibited properties lower than neat specimens. Our studies lead us to believe that nanofibres, are not effective in increasing strength of syntactic foams. For substantial

improvement, the reinforcement must be accompanied with other inherently tough fillers, which should interact strongly with the matrix.

CHAPTER 5

REFERENCES

1. Pinisetty, D., V.C. Shunmugasamy, and N. Gupta, *6 - Hollow Glass Microspheres in Thermosets—Epoxy Syntactic Foams*, in *Hollow Glass Microspheres for Plastics, Elastomers, and Adhesives Compounds*, S.E. Amos and B. Yalcin, Editors. 2015, William Andrew Publishing: Oxford. p. 147-174.
2. Huang, R. and P. Li, *Elastic behaviour and failure mechanism in epoxy syntactic foams: The effect of glass microballoon volume fractions*. *Composites Part B: Engineering*, 2015. **78**(0): p. 401-408.
3. Poveda, R.L., G. Dorogokupets, and N. Gupta, *Carbon nanofiber reinforced syntactic foams: Degradation mechanism for long term moisture exposure and residual compressive properties*. *Polymer Degradation and Stability*, 2013. **98**(10): p. 2041-2053.
4. Zhang, L. and J. Ma, *Effect of carbon nanofiber reinforcement on mechanical properties of syntactic foam*. *Materials Science and Engineering: A*, 2013. **574**(0): p. 191-196.
5. Gupta, N., et al., *Correlation of Processing Methodology to the Physical and Mechanical Properties of Syntactic Foams With and Without Fibers'*, in *Materials Characterization 1999*. p. 271-277.

6. Asif, A., V.L. Rao, and K.N. Ninan, *Nanoclay reinforced thermoplastic toughened epoxy hybrid syntactic foam: Surface morphology, mechanical and thermo mechanical properties*. Materials Science and Engineering: A, 2010. **527**(23): p. 6184-6192.
7. Maharsia, R., N. Gupta, and H.D. Jerro, *Investigation of flexural strength properties of rubber and nanoclay reinforced hybrid syntactic foams*. Materials Science and Engineering: A, 2006. **417**(1–2): p. 249-258.
8. Bunn, P. and J.T. Mottram, *Manufacture and Compression Properties of Syntactic Foams*. Composites, 1993. **24**: p. 565-571.
9. John, B. and C.P. Reghunadhan Nair, *13 - Syntactic Foams*, in *Handbook of Thermoset Plastics (Third Edition)*, H. Dodiuk and S.H. Goodman, Editors. 2014, William Andrew Publishing: Boston. p. 511-554.
10. Landrock, A.H., *5 - Miscellaneous and specialty foams: Epoxy Foams, Polyester Foams, Silicone Foams, Urea-Formaldehyde Foams, Polybenzimidazole, Foams, Polyimide Foams, Polyphosphazene Foams, and Syntactic Foams*, in *Handbook of Plastic Foams*, A.H. Landrock, Editor. 1995, William Andrew Publishing: Park Ridge, NJ. p. 253-266.
11. Ferguson, J.B., et al., *Al–Al₂O₃ syntactic foams—Part II: Predicting mechanical properties of metal matrix syntactic foams reinforced with ceramic spheres*. Materials Science and Engineering: A, 2013. **582**(0): p. 423-432.
12. Song, B., et al., *Confinement effects on the dynamic compressive properties of an epoxy syntactic foam*. Composite Structures, 2005. **67**(3): p. 279-287.
13. Zhang, L. and J. Ma, *Effect of coupling agent on mechanical properties of hollow carbon microsphere/phenolic resin syntactic foam*. Composites Science and Technology, 2010. **70**(8): p. 1265-1271.
14. Labella, M., et al., *Mechanical and thermal properties of fly ash/vinyl ester syntactic foams*. Fuel, 2014. **121**(0): p. 240-249.
15. Pellegrino, A., et al., *The mechanical response of a syntactic polyurethane foam at low and high rates of strain*. International Journal of Impact Engineering, 2015. **75**(0): p. 214-221.
16. Mae, H., M. Omiya, and K. Kishimoto, *Effects of strain rate and density on tensile behavior of polypropylene syntactic foam with polymer microballoons*. Materials Science and Engineering: A, 2008. **477**(1–2): p. 168-178.
17. Lehmus, D., et al., *Quasi-static and Dynamic Mechanical Performance of Glass Microsphere- and Cenosphere-based 316L Syntactic Foams*. Procedia Materials Science, 2014. **4**(0): p. 383-387.
18. Shah, D.U., F. Vollrath, and D. Porter, *Silk cocoons as natural macro-balloon fillers in novel polyurethane-based syntactic foams*. Polymer, 2015. **56**(0): p. 93-101.
19. S.R, S., et al., *in Polymer Synthesis and Characterization*. Academic Press, San Diego, 1998: p. 61-67.
20. May, C.A. and Ed., *Epoxy Resins Chemistry and Technology*, Marcel Dekker, New York, . 1988.
21. D, L., et al., *Glass fibre reinforced thermoplastic moulding compositions based on polyesters and graft polymers : (BASF Aktiengesellschaft, Ludwigshafen, FRG) US Pat 4968731 (6 November 1990)*. Composites, 1992. **23**(6): p. 467.
22. Alonso, M.V., M.L. Auad, and S. Nutt, *Short-fiber-reinforced epoxy foams*. Composites Part A: Applied Science and Manufacturing, 2006. **37**(11): p. 1952-1960.
23. Huang, Y.-J., L. Vaikhanski, and S.R. Nutt, *3D long fiber-reinforced syntactic foam based on hollow polymeric microspheres*. Composites Part A: Applied Science and Manufacturing, 2006. **37**(3): p. 488-496.
24. Zegeye, E., A.K. Ghamsari, and E. Woldesenbet, *Mechanical properties of graphene platelets reinforced syntactic foams*. Composites Part B: Engineering, 2014. **60**(0): p. 268-273.
25. Huang, Z.-M., et al., *A review on polymer nanofibers by electrospinning and their applications in nanocomposites*. Composites Science and Technology, 2003. **63**: p. 2223-2253.

26. Frenot, A. and I.S. Chronakis, *Polymer nanofibers assembled by electrospinning*. Current Opinion in Colloid and Interface Science, 2003. **8**: p. 64-75.
27. He, M., et al., *Fibrous guided tissue regeneration membrane loaded with anti-inflammatory agent prepared by coaxial electrospinning for the purpose of controlled release*. Applied Surface Science, 2015. **335**(0): p. 121-129.
28. Pham, Q.P., Upma Sharma, and A.G. Mikos, *Electrospinning of Polymeric Nanofibers for Tissue Engineering Applications: A Review*. Tissue Engineering, 2006. **12**.
29. Abdelgawad, A.M., S.M. Hudson, and O.J. Rojas, *Antimicrobial wound dressing nanofiber mats from multicomponent (chitosan/silver-NPs/polyvinyl alcohol) systems*. Carbohydrate Polymers, 2014. **100**(0): p. 166-178.
30. Li, Y., Z. Huang, and Y. Lü, *Electrospinning of nylon-6,66,1010 terpolymer*. European Polymer Journal, 2006. **42**(7): p. 1696-1704.
31. Yang, E., X. Qin, and S. Wang, *Electrospun crosslinked polyvinyl alcohol membrane*. Materials Letters, 2008. **62**(20): p. 3555-3557.
32. Khatri, Z., et al., *UV-responsive polyvinyl alcohol nanofibers prepared by electrospinning*. Applied Surface Science, 2015. **342**(0): p. 64-68.
33. Fashandi, H. and M. Karimi, *Pore formation in polystyrene fiber by superimposing temperature and relative humidity of electrospinning atmosphere*. Polymer, 2012. **53**(25): p. 5832-5849.
34. Elsabee, M.Z., H.F. Naguib, and R.E. Morsi, *Chitosan based nanofibers, review*. Materials Science and Engineering: C, 2012. **32**(7): p. 1711-1726.
35. Avinash, B., et al., *Electrospinning of polymer nanofibers: Effects on oriented morphology, structures and tensile properties*. Composites Science and Technology 2010. **70**: p. 703-718.
36. NIKHIL, G., et al., *Applications of Polymer Matrix Syntactic Foams*. JOM, 2014. **66**(2).
37. L.E, M. and M. D.H., *AMPTIAC Q*. 2004. **8**(67).
38. Chen.M.Y., et al., *SPIE Proc.,Optic. Mater. Struct. Technol. (Bellingham, W, . 2009. IV p. p. 74250S- 1-9*.
39. ASTM, C.-. *Standard test method for flatwise compressive properties of sandwich cores*. ASTM International, West Conshohocken, PA. 1998.
40. Raghu, P., S. Kunigal, and J.R. Larry, *Energy Absorption Performance of Eco-Core – A Syntactic Foam*American Institute of Aeronautics and Astronautics.
41. Askeland, D.R., et al., *The science and engineering of materials*. 1996: Chapman & Hall.
42. M.V., A., A. M.L., and Nutt.S, *Short-fiber-reinforced epoxy foams*Composites: Part A, 2006. **37**: p. 1952-1960.
43. Bergshoef, M.M. and G. Vancso, *Journal of Advanced Materials* 1999. **11**(362.).
44. Mrinal, C.S. and N. Sabrina, *Nanoclay-Reinforced Syntactic Foams: Flexure and Thermal Behavior*Polymer Composites, 2010.